# NATIONAL ADVISORY COMMITTEE FOR AERONAUTICS

**TECHNICAL NOTE 2387**

## THREE-DIMENSIONAL UNSTEADY LIFT PROBLEMS IN HIGH-SPEED FLIGHT - THE TRIANGULAR WING

By Harvard Lomax, Max. A. Heaslet,
and Franklyn B. Fuller

Ames Aeronautical Laboratory
Moffett Field, Calif.




Washington
June 1951

NATIONAL ADVISORY COMMITTEE FOR AERONAUTICS

TECHNICAL NOTE 2387

# THREE-DIMENSIONAL UNSTEADY LIFT PROBLEMS IN HIGH-SPEED FLIGHT - THE TRIANGULAR WING

By Harvard Lomax, Max. A. Heaslet,
and Franklyn B. Fuller

## SUMMARY

The indicial lift and pitching-moment coefficients are derived for flat-plate triangular wings traveling at supersonic speeds. The coefficients are determined for angle-of-attack distributions corresponding to sinking wings and to pitching wings. The wing with supersonic edges is completely analyzed, and the wing with subsonic edges is partially analyzed, the solution in this case being completed for very narrow wings by an application of slender wing theory. In the case of the supersonic edges, a comparison is made with known two-dimensional results and also with the results for the same triangular wing in reversed flow.

## INTRODUCTION

The wing of triangular plan form has received considerable attention in the steady-state theory of three-dimensional wings in a supersonic stream. The purpose of the present report is to determine the aerodynamic characteristics of a triangular wing in supersonic unsteady motion.

There are several simple types of unsteady motion on which the analysis can be based. The so-called indicial motion, in which the velocity undergoes a discontinuous change at $t'=0$, will be considered here. (See also references 1 and 2.) It is possible to conceive the physical situation in two slightly different ways. For one, it can be supposed that the wing has been traveling at the constant velocity $V_o$ for an infinitely long time and then, at $t'=0$, starts suddenly to sink without pitching motion (or to pitch without sinking) while maintaining the forward velocity $V_o$. On the other hand, the wing may be considered to be at rest in still air until at $t'=0$ it starts suddenly either to sink or to pitch and, at the same instant, attains the forward velocity $V_o$. The latter physical picture will be used in this report. Problems of unsteady motion can also be approached with the initial assumption that the velocity potential depends harmonically on the time. (See reference 3.) These two approaches are quite compatible in that they

can be related through the use of superposition methods (Duhamel's integral, Fourier's integral) of the operational calculus.

The question of whether the coordinate system should move with the wing or remain fixed is also of some importance. (See reference 4 for a discussion.) The latter alternative, that is, where the wing moves away from the coordinate system, was chosen for this report because the velocity potential $\Phi$ in this case satisfies the wave equation

$$\Phi_{xx} + \Phi_{yy} + \Phi_{zz} - \frac{1}{a_o^2}\Phi_{t't'} = 0$$

where $x,y,z$ are Cartesian coordinates, $t'$ is time, and $a_o$ is the speed of sound in the undisturbed medium. The fact that the equation has this form is helpful in establishing analogs between steady and nonsteady motions, and these analogs are of considerable help in the solution of certain problems.

The boundary conditions to be considered correspond to the problem of the flat sinking wing (angle-of-attack distribution uniform over the plan form) and to the flat pitching wing (angle of attack varies linearly with chordwise distance) in indicial motion. First, the loading on a flat triangular wing with supersonic edges undergoing an indicial sinking motion is determined. Then a simplified method is developed whereby total lift and pitching-moment coefficient for the wing with supersonic edges may be obtained. These quantities are determined as functions of time, for both sinking and pitching wings.

Lastly, the triangular wing with subsonic edges is partially analyzed, and an approximate method for very slender wings is used to complete the determination of loading. The analog method, mentioned previously, is here of great value. Lift and pitching-moment coefficients for the sinking and pitching slender triangular wing are determined.

## LIST OF IMPORTANT SYMBOLS

$a_o$ speed of sound in the free stream

$c_o$ root chord of triangular wing

$C_L$ lift coefficient $\left(\dfrac{\text{lift}}{\frac{1}{2}\rho_o V_o^2 S}\right)$

$C_{L_\alpha}$ indicial lift coefficient due to angle-of-attack change (without pitching) $\left(C_{L_\alpha} = \dfrac{\partial C_L}{\partial \alpha}\Big|_{\alpha=0}\right)$

$C_{L_q}'$ indicial lift coefficient due to pitching on a wing rotating about its leading edge or apex $\left(C_{L_q} = \frac{\partial C_L}{\partial \frac{c_o \dot{\theta}}{V_o}}\bigg|_{\dot{\theta}=0}\right)$

$C_m$ pitching-moment coefficient, positive when trailing edge tends to sink relative to leading edge

$C_{m_\alpha}'$ indicial pitching-moment coefficient due to angle-of-attack change (without pitching) measured about the leading edge or apex $\left(C_{m_\alpha}' = \frac{\partial C_m'}{\partial \alpha}\bigg|_{\alpha=0}\right)$

$C_{m_q}'$ indicial pitching-moment coefficient due to pitching measured about the leading edge or apex $\left(C_{m_q}' = \frac{\partial C_m'}{\partial \frac{c_o \theta}{V_o}}\bigg|_{\dot{\theta}=0}\right)$

$m$ cotangent of sweep angle ($\cot \Lambda$)

$M_o$ free-stream Mach number $\left(\frac{V_o}{a_o}\right)$

$P_o$ $\frac{M_o}{2\alpha s}\int_{-s}^{s} \frac{\Delta p}{q_o}\, dy$

$P_1$ $\frac{m M_o V_o}{2\dot{\theta} s^2}\int_{-s}^{s} \frac{\Delta p}{q_o}\, dy$

$\frac{\Delta p}{q_o}$ loading coefficient (pressure on the lower surface minus pressure on the upper surface divided by free-stream dynamic pressure)

$q_o$ free-stream dynamic pressure $\left(\frac{1}{2}\rho_o V_o^2\right)$

$q$ dimensionless rate of pitching $\left(\frac{c_o \dot{\theta}}{V_o}\right)$

$s$ local semispan of wing

$S$ wing area

$t'$ time

$t$ $a_o t'$

$t_o$ $\frac{t}{c_o}$

$u,v,w$ perturbation velocity components in the $x,y,z$ directions, respectively

$V_o$ free-stream velocity

$x,y,z$ Cartesian coordinates

$x_{c.p.}$ distance of center of pressure from wing apex

$\alpha$ angle of attack (angle between flight path and plane of wing), radians

$\beta$ $\sqrt{|1-M_o^2|}$

$\beta_e$ $\frac{1}{m\,M_o + \sqrt{1+m^2}}$

$\theta$ wing angle of pitch, relative to initial attitude, positive when trailing edge lies below leading edge

$\dot{\theta}$ wing rate of pitch, positive when trailing edge is sinking relative to leading edge $\left(\frac{d\theta}{dt'}\right)$

$\Lambda$ angle of sweep of leading edge, positive for sweepback

$\rho_o$ free-stream density

$\tau$ $\frac{t}{s}$

$\tau_o$ chord lengths traveled $\left(\frac{V_o t'}{c_o} \text{ or } M_o t_o\right)$

$\varphi$ perturbation velocity potential

$\Delta\varphi$ jump in potential across the $z=0$ plane $[\varphi(x,y,0^+) - \varphi(x,y,0^-)]$

Subscripts

$n$ component taken normal to the leading edge

$u$ positive side of the $z=0$ plane, or upper surface of a wing

# THE PROBLEM AND THE NATURE OF ITS SOLUTION

Consider a wing situated in still air and a Cartesian coordinate system with origin on the leading edge at the point of wing symmetry. At time equal to zero, the wing starts impulsively to move in a straight line with constant velocity away from the coordinate system which remains fixed relative to the still air at infinity. The load distribution on a wing undergoing such a motion is called the indicial loading. Similarly, the forces and moments which are based on this loading are given the adjective indicial. The partial differential equation that is satisfied by the velocity potential $\varphi$ for such a motion can be written

$$\varphi_{tt} - \varphi_{xx} - \varphi_{yy} - \varphi_{zz} = 0 \tag{1}$$

which is the normalized form of the wave equation. In equation (1), x,y, and z are distances: x measured chordwise, y spanwise, and z vertically, and t is equal to $a_o t'$ where $a_o$ is the free-stream speed of sound and $t'$ is time.

The boundary conditions to which equation (1) is subject are dependent on the wing shape and motion. Adopting the assumptions of thin-airfoil theory, which are consistent with the assumptions already used in obtaining equation (1), it can be assumed that the slope of the wing surface, in the direction of motion, at any place and time is given by the ratio of the vertical velocity component in the $z=0$ plane to the wing's forward velocity component. For a flat plate, then, the following conditions are to be satisfied:

1. The vertical velocity $\varphi_z$ is a linear function of x, the coefficients of which depend upon the angle of attack and rate of pitch, over the portion of the xy plane occupied by the wing at any given time.

2. No perturbations exist at infinity.

3. There are no discontinuities in the velocity potential except over the region occupied by the wing and its vortex wake.

The problem has now been expressed as one of finding, for prescribed boundary conditions, a solution to the wave equation. It is often desirable to express the solution in terms of the loading coefficient rather than the potential function or velocity components. This coefficient can be written in its linearized form as

$$\frac{\Delta p}{q_o} = \frac{2}{V_o M_o} \frac{\partial \Delta \varphi}{\partial t} \tag{2}$$

The solution of the problem without further restrictions has, in general, not been obtained, although it can be shown that the boundary conditions for any wing in unsteady motion can be satisfied by a suitable superposition of sources and doublets (reference 4). However, the solution for wings with all supersonic edges can be written as a double integral of sources having intensities determined by the local slope of the wing. Hence, for a flat surface at constant angle of attack and not pitching,

$$\varphi(x,y) = \frac{V_o \alpha}{2\pi} \int_{S_a} \int \frac{1}{r} \, dx_1 dy_1 \tag{3}$$

where $S_a$ is the outline of the region of sources which can, at a given time, affect the point $x,y$ at which the potential is being determined, $r$ equals $\sqrt{(x-x_1)^2 + (y-y_1)^2}$, and $\alpha$ is the angle of attack of the wing. The area $S_a$ has been termed the acoustic plan form and a discussion of its significance is given in reference 4.

The solution for the triangular wing with subsonic edges can be obtained in certain regions, but in others the problem reverts to the solution of a double integral equation involving time and the two surface dimensions of the wing. If the triangular wing is slender, an approximate method for finding the pressure over the entire wing can be used. This method is to neglect the streamwise velocity gradients in comparison with the gradients in the plane normal to the free stream and also in comparison with the term $\varphi_{tt}$. There results for the partial differential equation governing the flow field (equation (1)) the wave equation of one lower dimension, namely,

$$\varphi_{tt} - \varphi_{yy} - \varphi_{zz} = 0 \tag{4}$$

As will be developed later, the boundary conditions become the same as for a rectangular flat plate of very low aspect ratio inclined at angle of attack to a free stream with a Mach number equal to $\sqrt{2}$. This analogy with the steady-state lifting-surface problem is useful since solutions to the latter problem have been obtained.

The indicial lift and pitching-moment coefficients will be determined for wings with two different vertical velocity distributions. The first is the case in which the boundary condition is

$$w_u = \varphi_z \Big|_{z=0} = -V_o \alpha$$

where $\alpha$ is the angle of attack, and $w_u$ is constant over the plan form. This case is referred to as that of the sinking wing. The other boundary-value problem considered is the one corresponding to a flat wing pitching at a constant rate about its leading edge or apex. The boundary conditions have the form

$$w_u = \varphi_z\big|_{z=0} = -\dot{\theta}\ (x+M_0t)$$

where $\theta$ is the constant rate of pitch and $(x + M_0t)$ is the distance aft the leading edge or apex of the wing. The pitching velocity $\dot{\theta}$ is considered positive when the trailing edge of the wing sinks relative to the axis of rotation.

The difference between $\alpha$ and $\theta$ is illustrated in the sketch, where for clearness the motion is shown to be oscillatory rather than indicial. The angle of attack $\alpha$ is the angle between the flat wing surface and the line tangent to the flight path of the leading edge or apex of the wing. The angle $\theta$ is the angle between the flat wing surface and the horizontal (see part (a) of the sketch). Part (b) of the sketch shows a wing undergoing a sinusoidal angle-of-attack variation with a zero angle of pitch throughout the motion. Part (c) shows a wing undergoing a sinusoidal angle-of-pitch variation taken about the leading edge, with the angle of attack remaining zero.

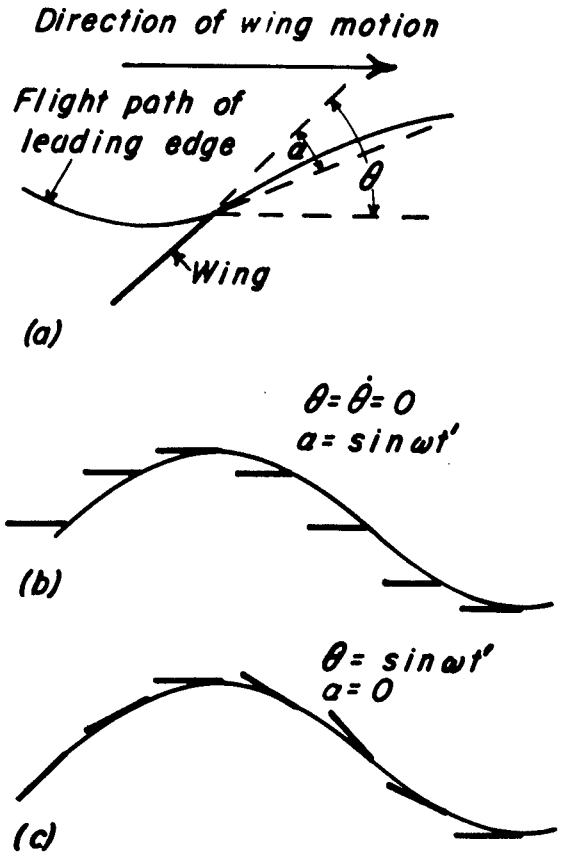


Although the lift and pitching-moment coefficients are given only for the two types of motion separately, it is possible, according to the linear theory, to combine them to simulate an arbitrary indicial maneuver consisting of both sinking and pitching motions. For such a case, the boundary condition becomes

$$w_u = -V_0\alpha - \dot{\theta}\ (x + M_0t)$$

If, furthermore, the desired maneuver is not indicial, the lift and pitching-moment coefficients may be determined by use of Duhamel's integral:

$$C_L = \frac{d}{dt'} \int_0^{t'} [C_{L_\alpha}(t'-\tau')\,\alpha(\tau') + C_{L_q}'(t'-\tau')q(\tau')]\,d\tau'$$

$$C_m = \frac{d}{dt'} \int_0^{t'} [C_{m_\alpha}'(t'-\tau')\alpha(\tau') + C_{m_q}'(t'-\tau')\,q(\tau')]\,d\tau'$$

where $\alpha(t')$ and $q(t')$ are the arbitrary motions $\left(q = \frac{c_o\dot{\theta}}{V_o}\right)$, $C_{L_\alpha}$, $C_{m_\alpha}'$, $C_{L_q}'$, and $C_{m_q}'$ are the indicial aerodynamic coefficients, and the primes on the coefficients indicate that the pitching motion is about, and the pitching moments are referred to, the leading edge or apex.

The position of the axis of pitching motion, and of the axis to which pitching-moment coefficient is referred, is of importance. In this report, these axes coincide in an axis normal to the root chord of the wing and passing through the wing leading edge or apex. However, it is often desired to transfer the pitching motion and moment calculation to other axes, and the formulas for such a transformation will be given here. Let the pitching motion refer to an axis lying a distance $ac_o$ back of the leading edge or apex, and let the pitching-moment coefficients refer to an axis $bc_o$ aft the leading edge or apex. The necessary transformation formulas are

$$C_{m_\alpha}\big|_b = C_{m_\alpha}' + b\,C_{L_\alpha}$$

$$C_{L_q}\big|_a = C_{L_q}' - a\,C_{L_\alpha}$$

$$C_{m_q}\big|_{a,b} = C_{m_q}' + b\,C_{L_q}' - a\,C_{m_\alpha}' - ab\,C_{L_\alpha}$$

where a prime on a quantity indicates that the pitching motion is about, and the pitching moments are measured about, an axis through the leading edge or apex of the wing. The quantity $q$ is the dimensionless rate of pitching, equal to $c_o\,\dot{\theta}/V_o$. The subscripts $a$ and $b$ mean, respectively, that the quantity in question refers to a pitching motion about an axis at a distance $ac_o$ aft the leading edge or apex, or that the pitching moments are measured about an axis $bc_o$ aft the leading edge or apex.

# WING WITH SUPERSONIC EDGES

## INDICIAL LOADING FOR SINKING WING

### Analysis

The seven regions.- The analytic expression for the indicial loading over the triangular wing has a different form in each of seven regions. These regions are determined by the positions of the various wave fronts relative to the wing plan form (fig. 1). For $t<0$ the wing is motionless, its leading edge lying along lines represented by the dashed lines in figure 1. At $t=0$ the wing starts suddenly to move, and for $t>0$, travels forward at a constant speed $V_o$. After a certain time $t$ has elapsed, the wing has traveled to a new position, also shown in the figure. In this same interval of time, pressure impulses have traveled out in spherical waves from every point of the region which the wing has occupied. The trace on the wing of the sphere starting from the wing apex at $t=0$ forms the external boundary of region 7. The area outside this circle and within the traces of the cylindrical waves (the envelopes of the spherical waves) generated by the leading edges at $t=0$ forms region 4. Region 5 is formed by the overlapping of these cylindrical waves, and the solution for loading within it can be found by a suitable superposition of the solutions for regions 3 and 4. Region 1 lies between the cylinder trace on the wing and the leading-edge position at time $t$; the loading in this region cannot be affected by the manner in which the wing started its motion since it lies outside the starting cylindrical waves. Hence, the loading in region 1 is the same as that on a swept wing flying at a steady supersonic speed. The solution in region 2 can also be obtained from steady-state lifting-surface theory, but, whereas in region 1 the field is two-dimensional (i.e., invariant with distance measured parallel to the leading edge), in region 2 the field is conical. Region 6 is formed by the overlapping of regions 2 and 4. Finally, region 3 is that area completely unaffected by waves from the wing edges. In the following subdivisions the analysis of each of the separate regions will be discussed.

Region 1: The loading in region 1 of figure 1 is equal to the loading on a two-dimensional flat plate moving at a constant velocity given by the component of stream velocity normal to the leading edge of the triangular wing. Since this component is supersonic, the loading is of the Ackeret type and is given by

$$\left(\frac{\Delta p}{q_n}\right)_1 = \frac{4\alpha_n}{\beta n}$$

But since $V_n = V_o \cos \Lambda$ where $\Lambda$ is the angle of sweep (see fig. 2),

$$q_n = q_o \cos^2\Lambda$$

$$c_n = \alpha \sec \Lambda$$

$$M_n = M_o \cos \Lambda$$

$$\beta_n = \sqrt{M_o^2 \cos^2\Lambda - 1}$$

and

$$\left(\frac{\Delta p}{q_o}\right)_1 = \frac{4\alpha}{\sqrt{M_o^2 - \sec^2\Lambda}}$$

Finally, if $\operatorname{ctn} \Lambda = m$

$$\left(\frac{\Delta p}{q_o}\right)_1 = \frac{4\alpha m}{\sqrt{\beta^2 m^2 - 1}} \tag{5}$$

where $\beta = \sqrt{M_o^2 - 1}$.

Region 2: The steady-state loading on a triangular wing with supersonic edges has been given by several authors (see, for convenience, reference 5) so the expression for the loading in region 2 can be written immediately for the coordinate system shown in figure 2 as

$$\left(\frac{\Delta p}{q_o}\right)_2 = \frac{4\alpha m}{\pi\sqrt{\beta^2 m^2 - 1}} \left\{ \pi + \arcsin \frac{\beta^2 my - (x + M_o t)}{\beta[m(x + M_o t) - y]} - \right.$$

$$\left. \arcsin \frac{\beta^2 my + (x + M_o t)}{\beta[M(x + M_o t) + y]} \right\} \tag{6}$$

Region 3: Since region 3 is unaffected by the edges of the wing the solution for the loading therein can be written as in reference 6

$$\left(\frac{\Delta p}{q_o}\right)_3 = \frac{4\alpha}{M_o} \tag{7}$$

Region 4: The solution for loading in region 4 can be obtained from consideration of a two-dimensional wing starting from rest and moving with velocity $V_n$ normal to its leading edge. This problem

has been treated in reference 6 and the solution written there can be written for the right-hand side of figure 1 as

$$\left(\frac{\Delta p}{q_n}\right)_4 = \frac{4\alpha_n}{\pi\beta_n}\left[\arccos\frac{M_n x_n + t}{x_n + M_n t} + \frac{\sqrt{M_n^2-1}}{M_n}\left(\frac{\pi}{2} + \arcsin\frac{x_n}{t}\right)\right]$$

where the notation, as defined by the sketch, is

$$x_n = x\cos\Lambda - y\sin\Lambda$$

$$y_n = x\sin\Lambda + y\cos\Lambda$$

and since

$$\operatorname{ctn}\Lambda = m,\quad \sin\Lambda = \frac{1}{\sqrt{1+m^2}},$$

$$\cos\Lambda = \frac{m}{\sqrt{1+m^2}}$$

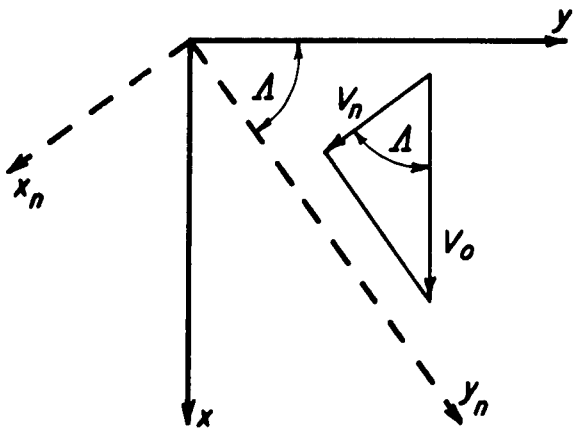


Then

$$x_n = \frac{mx-y}{\sqrt{1+m^2}}$$

$$y_n = \frac{x+my}{\sqrt{1+m^2}}$$

The equation for loading now becomes, in the coordinate system of figure 2,

$$\left(\frac{\Delta p}{q_o}\right)_4 = \frac{4\alpha m}{\pi\sqrt{\beta^2m^2-1}}\left[\arccos\frac{mM_o(mx-|y|)+t(1+m^2)}{\sqrt{1+m^2}\,(mx-|y|+mM_o t)} + \frac{\sqrt{\beta^2m^2-1}}{mM_o}\left(\frac{\pi}{2} + \arcsin\frac{mx-|y|}{t\sqrt{1+m^2}}\right)\right] \tag{8}$$

Region 5: The solution for loading in region 5 can be obtained by superposition of the solutions for regions 3 and 4. If the solutions for the two sides of region 4 (obtained from equation 8) are added, the result gives a value of $w_u$ of twice the required amount in region 5, as well as undesirable pressures off the wing. However, subtraction from this sum of the solution for region 3 (equation 7) reduces the downwash $w_u$ to the proper value, and also cancels the excess pressures. The resulting expression can be written

$$\left(\frac{\Delta p}{q_o}\right)_5 = \frac{4\alpha m}{\pi\sqrt{\beta^2m^2-1}}\left[\arccos\frac{mM_o(mx-y)+(1+m^2)t}{\sqrt{1+m^2}\,(mx-y+mM_ot)}+\right.$$

$$\arccos\frac{mM_o(mx+y)+(1+m^2)t}{\sqrt{1+m^2}\,(mx+y+mM_ot)}+$$

$$\left.\frac{\sqrt{\beta^2m^2-1}}{mM_o}\left(\arcsin\frac{mx+y}{\sqrt{1+m^2}\,t}+\arcsin\frac{mx-y}{\sqrt{1+m^2}\,t}\right)\right] \quad (9)$$

Region 6: The loading in region 6 can also be calculated by superposition. To find the loading in this case, add the solutions for regions 2 and 4 (equations (6) and (8)) and subtract the solution for region 1 (equation (5)). There results

$$\left(\frac{\Delta p}{q_o}\right)_6 = \frac{4\alpha m}{\pi\sqrt{\beta^2m^2-1}}\left\{\arcsin\frac{\beta^2my-(x+M_ot)}{\beta[m(x+M_ot)-y]}-\arcsin\frac{\beta^2my+(x+M_ot)}{\beta[m(x+M_ot)+y]}+\right.$$

$$\arccos\frac{mM_o(mx-|y|)+t(1+m^2)}{(mx-|y|+mM_ot)\sqrt{1+m^2}}+$$

$$\left.\frac{\sqrt{\beta^2m^2-1}}{mM_o}\left(\frac{\pi}{2}+\arcsin\frac{mx-|y|}{t\sqrt{1+m^2}}\right)\right\} \quad (10)$$

Region 7: The solution for the loading in region 7 can be obtained by means of equation (3). The analysis used in finding the solution in this region is not difficult but the algebra is rather involved. It is useful at this point to introduce polar coordinates (see sketch) such that

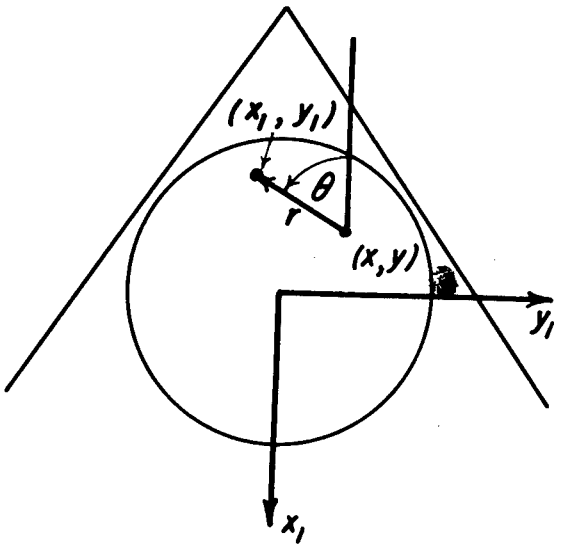


$$x-x_1 = r\cos\theta$$

$$y-y_1 = r\sin\theta$$

$$dx_1dy_1 = r\,dr\,d\theta \quad (11)$$

From equation (11), equation (3) can be written in the form

$$\varphi = \frac{V_o\alpha}{2\pi}\int_{S_a}\int dr d\theta \quad (12)$$

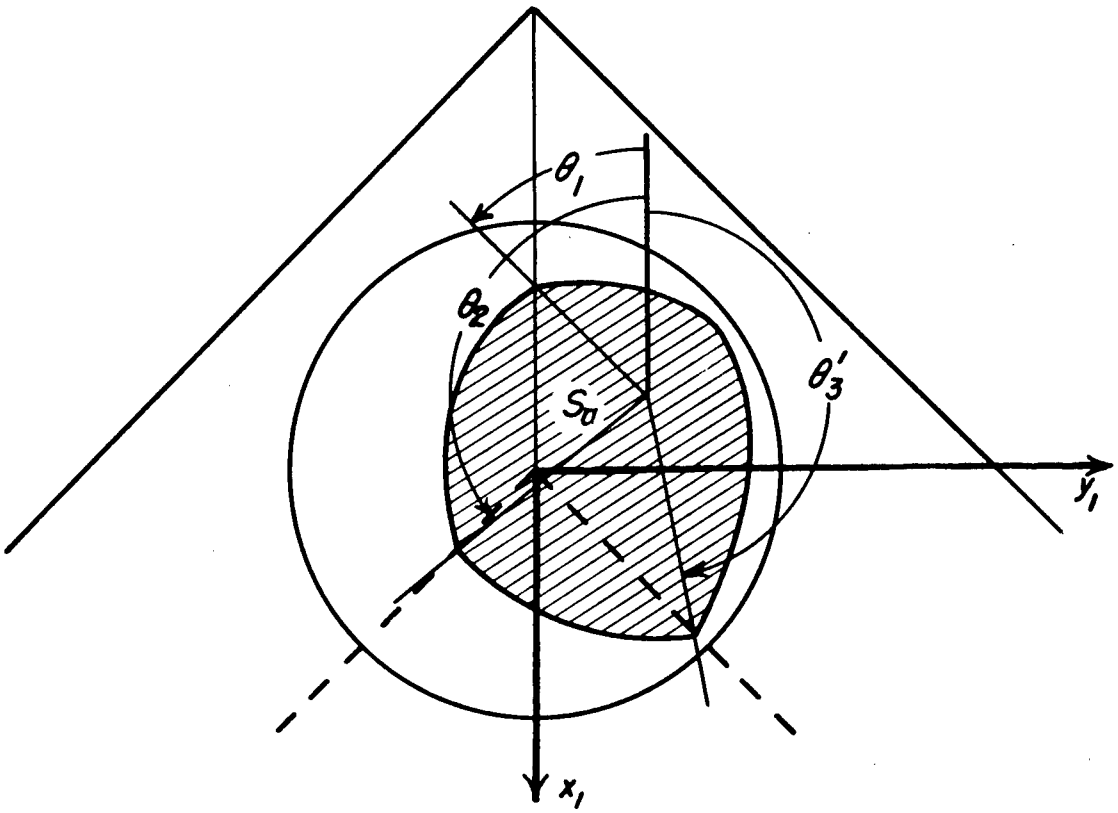


The acoustic plan form for points in region 7 is the region bounded by three curves as indicated in the sketch. The arc between $\theta_1$ and $\theta_2$ is determined by eliminating T between the equations

$$r^2 = (t - T)^2$$

(the equation for the inverse sound waves) and the equation for the left leading edge

$$y_1 = -m(x_1 + M_0T)$$

The arc between $\theta_3$ and $\theta_1$ is found by determining the acoustic intersection (eliminating T) of the right leading edge with the inverse sound wave; and, finally, the arc between $\theta_2$ and $\theta_3$ is given by the equation r=t. The equations of these arcs can be written in polar coordinates as

$$r = \frac{m(x+M_o t)+y}{m\cos\theta+mM_o+\sin\theta} \; ; \; \theta_1 \le \theta \le \theta_2$$

$$r = t; \quad \theta_2 \le \theta \le \theta_3$$

$$r = \frac{m(x+M_o t)-y}{m\cos\theta+mM_o-\sin\theta} \; ; \begin{cases} 0 \le \theta \le \theta_1 \\ \theta_3 \le \theta \le 2\pi \end{cases}$$

Using these expressions, equation (12) reduces to

$$\varphi = \frac{V_o\alpha}{2\pi}\int_{\theta_1}^{\theta_2}\frac{m(x+M_o t)+y}{m\cos\theta+mM_o+\sin\theta}\,d\theta + \frac{V_o\alpha}{2\pi}\int_{\theta_2}^{\theta_3} t\,d\theta + \frac{V_o\alpha}{2\pi}\int_{\theta_3}^{\theta_1}\frac{m(x+M_o t)-y}{m\cos\theta+mM_o-\sin\theta}\,d\theta$$

and taking the partial derivative with respect to $t$ (to determine the loading according to equation (2)) one finds[1]

$$\left(\frac{\Delta p}{q_o}\right)_7 = \frac{2\alpha\, m}{\pi}\int_{\theta_1}^{\theta_2}\frac{d\theta}{mM_o + m\cos\theta+\sin\theta} + \frac{2\alpha}{\pi M_o}\int_{\theta_2}^{\theta_3} d\theta + \frac{2\alpha\, m}{\pi}\int_{\theta_3}^{\theta_1}\frac{d\theta}{mM_o + m\cos\theta-\sin\theta} \qquad (13)$$

In evaluating this equation, the following integral is used:

for $-\pi \le \theta \le \pi$

$$\int \frac{d\theta}{mM_o + m\cos\theta \pm \sin\theta} = \frac{2}{\sqrt{\beta^2m^2-1}}\arctan\frac{m(M_o-1)\tan(\theta/2)\pm 1}{\sqrt{\beta^2m^2-1}} \qquad (14)$$

[1]The limits $\theta_1$, $\theta_2$, and $\theta_3$ are all functions of $t$ but in moving the partial derivative through the integral sign the terms involving $\partial\theta_1/\partial t$, $\partial\theta_2/\partial t$, and $\partial\theta_3/\partial t$ all cancel one another.

Since equation (14) is valid only in the interval $-\pi \leq \theta \leq \pi$, care must be exercised in applying it because the angle $\theta_3$ may be greater than $\pi$ (as in the preceding sketch). In case $\pi \leq \theta_3$, it is convenient to introduce the angle $\theta_3' = \theta_3 - 2\pi$. The expression for $\Delta p/q_0$ can then be written in two forms, according as $\theta_3$ is less than or greater than $\pi$:

for $y \geq 0$, $\theta_3 \leq \pi$

$$\left(\frac{\Delta p}{q_0}\right)_7 = \frac{4\alpha m}{\pi\sqrt{\beta^2m^2-1}}\left[\pi + \arctan\frac{m(M_0-1)\tan(\theta_1/2)-1}{\sqrt{\beta^2m^2-1}} - \arctan\frac{m(M_0-1)\tan(\theta_1/2)+1}{\sqrt{\beta^2m^2-1}} + \arctan\frac{m(M_0-1)\tan(\theta_2/2)+1}{\sqrt{\beta^2m^2-1}} - \arctan\frac{m(M_0-1)\tan(\theta_3/2)-1}{\sqrt{\beta^2m^2-1}}\right] + \frac{2\alpha}{\pi M_0}(\theta_3 - \theta_2) \qquad (15a)$$

for $y \geq 0$, $\pi \leq \theta_3$

$$\left(\frac{\Delta p}{q_0}\right)_7 = \frac{4\alpha m}{\pi\sqrt{\beta^2m^2-1}}\left[\arctan\frac{m(M_0-1)\tan(\theta_1/2)-1}{\sqrt{\beta^2m^2-1}} - \arctan\frac{m(M_0-1)\tan(\theta_1/2)+1}{\sqrt{\beta^2m^2-1}} + \arctan\frac{m(M_0-1)\tan(\theta_2/2)+1}{\sqrt{\beta^2m^2-1}} - \arctan\frac{m(M_0-1)\tan(\theta_3'/2)-1}{\sqrt{\beta^2m^2-1}}\right] + \frac{2\alpha}{\pi M_0}(\theta_3' - \theta_2 + 2\pi) \qquad (15b)$$

where

$$\theta_1 = \arccos\frac{-M_0 y^2 + (x+M_0t)\sqrt{(x+M_0t)^2-\beta^2y^2}}{y^2 + (x+M_0t)^2}$$

$(0 < \theta_1 < \pi)$

$$\theta_2 = \arccos\frac{m(y+mx) - \sqrt{(1+m^2)t^2 - (y+mx)^2}}{(1+m^2)t}$$

$(0 < \theta_2 < \pi)$

$$\theta_3 = \arccos \frac{-m(y-mx) - \sqrt{(1+m^2)t^2 - (y-mx)^2}}{(1+m^2)\,t}$$

$$\theta_3' = \theta_3 - 2\pi \quad (\text{if } \pi \leq \theta_3)$$

The limitation on $\theta_3$ can be given both an analytic and geometric interpretation. Thus, equation (15(a)) applies for $0 \leq m(x+t) \leq y$ and equation (15(b)) applies for $0 \leq y \leq m(x+t)$. These regions are shown in the accompanying sketch. Because of the geometrical symmetry about the x axis, equations (15) suffice for the determination of loading throughout region 7.

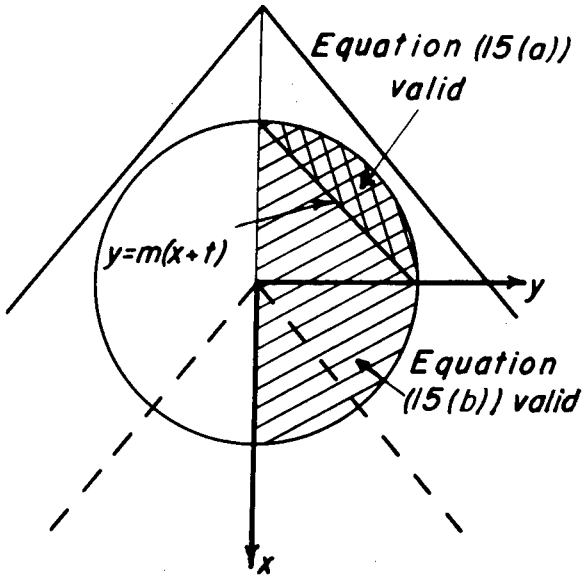


## Discussion of Results

Plots of the load distribution on the sinking triangular wing with supersonic edges are shown in figure 3, and an isometric drawing of the

loading on the right panel appears in the sketch. The positions of the spanwise sections were chosen so that each of the regions 1 through 7 is represented. It is to be noted that the results for region 7 show no unusual characteristics, but fit in well with those for the adjoining regions. In general, the distribution is similar to the steady-state loading on a triangular wing.

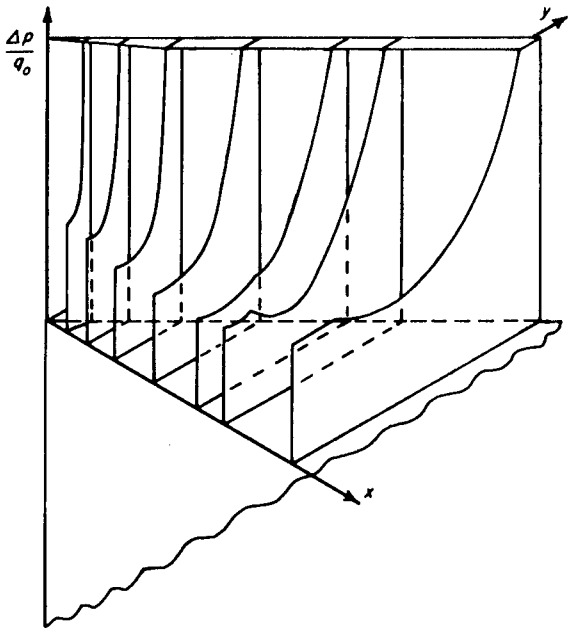


## INDICIAL LIFT AND PITCHING MOMENT

### Analysis

Methods of solution.- If a detailed knowledge of the load distribution is not required, but only the total values of lift and moment need be known, analyses much simpler than the one presented in the previous section can be employed. These methods, however, not only require the edges of the wing to be supersonic, but also require the trailing edge to be straight and normal to the free-stream direction. One such simple method has been presented in reference 4. It involves the integration over the three-dimensional plan form of longitudinal strips, or elements, which carry the two-dimensional values of loading as a function of time. The results presented in the present section can be derived by this method as well as by the method to be developed next.

Consider again equation (1) and integrate each term with respect to $y$ between the limits minus and plus infinity.[2] There results the equation

$$\int_{-\infty}^{\infty} \frac{\partial^2 \varphi}{\partial x^2}\,dy + \int_{-\infty}^{\infty} \frac{\partial^2 \varphi}{\partial y^2}\,dy + \int_{-\infty}^{\infty} \frac{\partial^2 \varphi}{\partial z^2}\,dy - \int_{-\infty}^{\infty} \frac{\partial^2 \varphi}{\partial t^2}\,dy = 0$$

If $y = y_l(x,z,t)$ and $y = y_r(x,z,t)$ are the equations of the Mach waves streaming back from the leading edges on the left and right sides of the wing, respectively, then, since $\varphi$ is continuous across these

[2]The basic idea for this solution was given by Prof. P. A. Lagerstrom in his lectures at the California Institute of Technology.

waves but $\varphi_x$, $\varphi_y$, $\varphi_z$, and $\varphi_t$ are not,

$$\frac{\partial^2}{\partial x^2}\int_{y_l}^{y_r}\varphi\,dy = \frac{\partial y_r}{\partial x}u_r - \frac{\partial y_l}{\partial x}u_l + \int_{y_l}^{y_r}\frac{\partial^2\varphi}{\partial x^2}\,dy$$

where $u_r$ and $u_l$ are the values of $u$ on the interior faces of the right and left Mach waves, respectively, and

$$\int_{y_l}^{y_r}\frac{\partial^2\varphi}{\partial y^2}\,dy = v_r - v_l$$

Values of the terms involving $w$ and $\varphi_t$ are similar to those involving $u$ so that finally, if

$$\Phi = \int_{y_l}^{y_r}\varphi\,dy \tag{16}$$

then

$$\frac{\partial^2\Phi}{\partial x^2} + \frac{\partial^2\Phi}{\partial z^2} - \frac{\partial^2\Phi}{\partial t^2} = \left(\frac{\partial y_r}{\partial x}u_r + \frac{\partial y_r}{\partial z}w_r - \frac{\partial y_r}{\partial t}\varphi_t - v_r\right) - \left(\frac{\partial y_l}{\partial x}u_l + \frac{\partial y_l}{\partial z}w_l - \frac{\partial y_l}{\partial t}\varphi_t - v_l\right)$$

The terms enclosed within the brackets in the last equation combine so that each bracketed quantity is zero. For the case of interest here, this is not difficult to show. Consider, for example, the right wedge. Then, since the equation of the wedge is

$$y_r = -z\sqrt{\beta^2m^2-1} + mx + mM_ot$$

and the value of the potential is the steady-state two-dimensional value given by the expression

$$\varphi_r = -w_u\frac{m(x+M_ot)-y-z\sqrt{\beta^2m^2-1}}{\sqrt{\beta^2m^2-1}}$$

the term

$$\left( \frac{\partial y_r}{\partial x} u_r + \frac{\partial y_r}{\partial z} w_r - \frac{\partial y_r}{\partial t} \varphi_t - v_r \right)$$

becomes

$$-w_u \left( m \frac{m}{\sqrt{\beta^2 m^2 - 1}} + \sqrt{\beta^2 m^2 - 1} - \frac{m^2 M_o^2}{\sqrt{\beta^2 m^2 - 1}} + \frac{1}{\sqrt{\beta^2 m^2 - 1}} \right)$$

and this is identically zero.[3]

Finally, therefore, equation (1) has been reduced in terms of equation (16) to

$$\Phi_{tt} - \Phi_{xx} - \Phi_{zz} = 0 \tag{17}$$

Consider next the boundary conditions for a triangular wing with supersonic edges. In the plane $z=0$, $\partial \Phi / \partial z$ becomes $\int_{-\infty}^{\infty} w_u dy$ where $w_u$ is the vertical induced velocity in the plane of the wing. Since the edges are supersonic, however, $w_u$ must be zero off the plan form of the wing and the integration need extend only over the plan form itself. Hence

$$\left( \frac{\partial \Phi}{\partial z} \right)_{z=0} = -2 V_o \alpha m \, (x + M_o t) \tag{18}$$

for the flat triangular wing at constant angle of attack and

$$\left( \frac{\partial \Phi}{\partial z} \right)_{z=0} = -2 \dot{\theta} m \, (x + M_o t)^2 \tag{19}$$

---

[3] It is not necessary to perform a direct calculation in order to prove the above result for arbitrary plan forms. The bracketed terms represent the directional derivative of the velocity potential taken along the so-called "conormal" of the foremost disturbance surface. Since $\varphi$ is constant on the surface, and since the conormal lies along the surface, the bracketed terms are zero.

for a flat triangular wing with a constant rate of pitch $\theta$ about its apex (positive $\dot{\theta}$ produces a downward motion of the trailing edge relative to the leading edge).

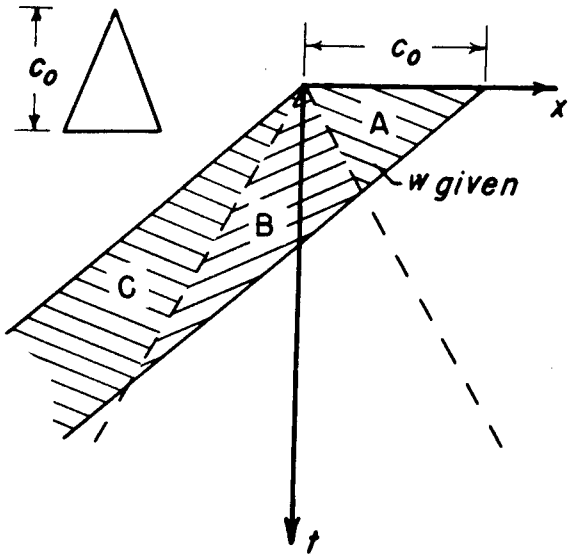


These boundary conditions are exactly like those studied in steady-state supersonic wing theory. In fact, the lifting-surface analog (shown on the sketch) is a wing tip of specified camber in a supersonic free stream having a Mach number equal to $\sqrt{2}$. The solution for the potential in the plane of the wing for this problem can therefore be written immediately as

$$(\Phi)_{z=0} = -\frac{1}{\pi}\int_{\sigma}\int \frac{\left(\frac{\partial \Phi}{\partial z}\right)_{z=0}}{\sqrt{(t-t_1)^2-(x-x_1)^2}}\,dt_1\,dx_1$$

where $\sigma$ is the portion of the area on the shaded surface in the sketch lying ahead of the forecone traces given by the equation $(t-t_1)^2 = (x-x_1)^2$. Using equation (2) for the loading coefficient, and introducing the following notation for the average spanwise loading

$$P_o = \frac{M_o}{2s\alpha}\int_{-s}^{s}\frac{\Delta p}{q_o}dy \quad \text{(sinking wing)} \qquad (20a)$$

$$P_1 = \frac{mM_oV_o}{2s^2\,\dot{\theta}}\int_{-s}^{s}\frac{\Delta p}{q_o}dy \quad \text{(pitching wing)} \qquad (20b)$$

where

$$s = m(x+M_0t) \tag{21}$$

it is found that

$$P_0 = \frac{4m}{\pi s}\frac{\partial}{\partial t}\int_\sigma\int \frac{(x_1+M_0t_1)\,dx_1dt_1}{\sqrt{(t-t_1)^2-(x-x_1)^2}} \tag{22}$$

$$P_1 = \frac{4m^2}{\pi s^2}\frac{\partial}{\partial t}\int_\sigma\int \frac{(x_1+M_0t_1)^2\,dx_1\,dt_1}{\sqrt{(t-t_1)^2-(x-x_1)^2}} \tag{23}$$

Wing with constant angle of attack (sinking wing).- The solution for the average load on a flat, supersonic-edged, triangular wing starting from rest at $t=0$ and flying at a constant speed and angle of attack is given by equation (22). With the transformations

$$x-x_1 = x_2$$

$$t-t_1 = t_2$$

this becomes

$$P_0 = \frac{4m}{\pi s}\frac{\partial}{\partial t}\int_\sigma\int dt_2dx_2\,\frac{\frac{s}{m}-x_2-M_0t_2}{\sqrt{t_2^2-x_2^2}}$$

This integral can be evaluated and gives for $x<t$ (region A)

$$P_0 = 4 \tag{24a}$$

for $-t \le x \le t$ (region B)

$$P_0 = \frac{4}{\pi}\left[\frac{\sqrt{t^2-x^2}}{x+M_0t} + \arccos\left(-\frac{x}{t}\right) + \frac{M_0}{\beta}\arccos\frac{t+M_0x}{x+M_0t}\right] \tag{24b}$$

and for $x<-t$ (region C)

$$P_0 = \frac{4M_0}{\beta} \tag{24c}$$

where the regions are shown in the preceding sketch. Equations (24) can also be obtained by integrating the equations for the loading given in

the preceding section. These integrations were carried out (in some regions numerically) and the results were found to agree with those of the present analysis.

It is now possible to write the equation for the indicial lift and pitching moment for a sinking wing:

$$C_{L_\alpha} = \frac{2}{S\,M_o} \int_{-M_o t}^{c_o - M_o t} m(x+M_o t)\, P_o\, dx \tag{25}$$

$$C_{m_\alpha}{}' = -\frac{2}{S\,c_o\,M_o} \int_{-M_o t}^{c_o - M_o t} m(x+M_o t)^2\, P_o\, dx \tag{26}$$

where $S$ is the wing area (equal to $mc_o^2$) and the prime indicates that the pitching moment is measured about the apex, the positive moment being one which causes the trailing edge to sink relative to the apex.

Combining equations (24) and (25) one finds for the first interval shown in the sketch

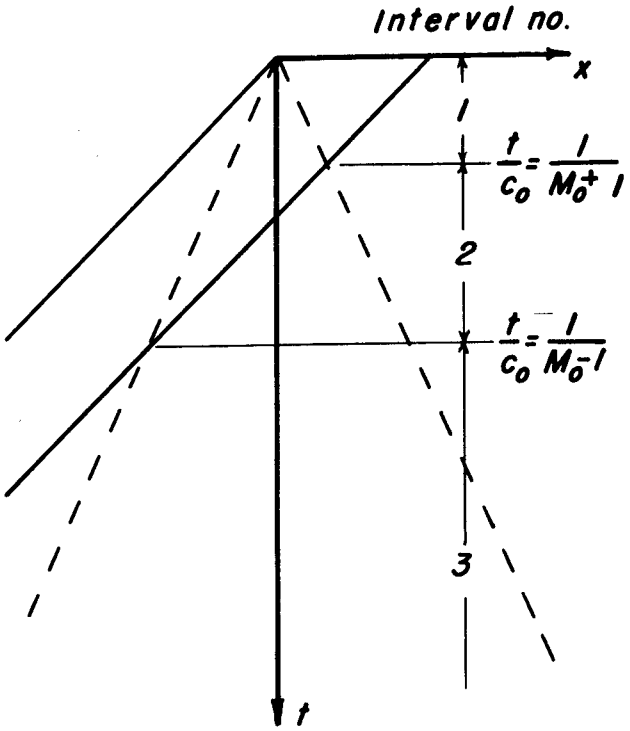

$$C_{L_\alpha} = \frac{2}{M_o c_o^2}\left\{ \int_{-Mt}^{-t} \frac{4M_o}{\beta}(x+M_o t)\,dx + \right.$$

$$\frac{4}{\pi}\int_{-t}^{t}(x+M_o t)\left[\frac{\sqrt{t^2-x^2}}{x+M_o t} + \arccos\left(-\frac{x}{t}\right) + \right.$$

$$\left.\left.\frac{M_o}{\beta}\arccos\frac{t+M_o x}{x+M_o t}\right]dx + \right.$$

$$\left.\int_{t}^{c_o-M_o t} 4(x+M_o t)\,dx\right\}$$

This equation integrates to give, if $t_o = t/c_o$,

for $0 \le t_o \le \frac{1}{M_o+1}$ (first interval)

$$C_{L_\alpha} = \frac{4}{M_o}\left(1 + \frac{1}{2}t_o^2\right) \tag{27a}$$

Similarly for $\frac{1}{M_o+1} \le t_o \le \frac{1}{M_o-1}$ (second interval)

$$C_{L_\alpha} = \frac{4}{\pi M_o}\left(1 + \frac{1}{2}t_o^2\right)\arccos\frac{M_o t_o - 1}{t_o} +$$

$$\frac{4}{\pi\beta}\arccos\left(M_o - t_o\beta^2\right) +$$

$$2\,\frac{3-M_o t_o}{\pi M_o}\sqrt{t_o^2 - (1-M_o t_o)^2} \tag{27b}$$

and for $\frac{1}{M_o-1} \le t_o$ (third interval)

$$C_{L_\alpha} = \frac{4}{\beta} \tag{27c}$$

In the same manner the values for $C_{m_\alpha}$ in the various intervals can be determined by combining equations (24) and (26). There results

for $0 \leq t_o \leq \frac{1}{M_o+1}$ (first interval)

$$C_{m_\alpha}' = -\frac{8}{3M_o}\left(1 + \frac{1}{2} M_o t_o^3\right) \tag{28a}$$

for $\frac{1}{M_o+1} \leq t_o \leq \frac{1}{M_o-1}$ (second interval)

$$C_{m_\alpha}' = -\frac{8}{\pi M_o}\left[\frac{1}{18}(8-M_o t_o - M_o^2 t_o^2 - 2t_o^2)\sqrt{t_o^2-(1-M_o t_o)^2} + \right.$$

$$\left. \frac{1}{6}(2+M_o t_o^3) \arccos\frac{M_o t_o - 1}{t_o} + \frac{M_o}{3\beta} \arccos(M_o - \beta^2 t_o)\right] \tag{28b}$$

and for $\frac{1}{M_o-1} \leq t_o$ (third interval)

$$C_{m_\alpha}' = -\frac{8}{3\beta} \tag{28c}$$

Numerical results for a Mach number of 2 will be presented in the discussion section.

Wing with linear angle-of-attack variation (pitching wing).- The solution for the average load on a flat, supersonic-edged, triangular wing flying at a constant speed and pitching at a uniform rate $\dot{\theta}$ about its apex is given by equation (23). With the transformation

$$x - x_1 = x_2$$

$$t - t_1 = t_2$$

this equation becomes

$$P_1 = \frac{4m^2}{\pi s^2} \frac{\partial}{\partial t} \int_\sigma \int \frac{\left(\frac{s}{m} - x_2 - M_o t_2\right)^2}{\sqrt{t_2^2 - x_2^2}} \, dt_2 \, dx_2$$

and the evaluation of this gives (for the regions defined for the sinking wing)

for $x \leq t$ (region A)

$$P_1 = 4\left[1 + \frac{1}{2}\left(\frac{t}{x+M_o t}\right)^2\right] \tag{29a}$$

for $-t \leq x \leq t$ (region B)

$$P_1 = \frac{4}{\pi}\left[\frac{1}{2}\frac{t^2+(x+M_o t)^2}{(x+M_o t)^2}\arccos\left(-\frac{x}{t}\right) + \frac{M_o}{\beta}\arccos\frac{t+M_o x}{x+M_o t} + \frac{1}{2}\frac{3x+2M_o t}{(x+M_o t)^2}\sqrt{t^2-x^2}\right] \tag{29b}$$

and for $x \leq -t$ (region C)

$$P_1 = \frac{4M_o}{\beta} \tag{29c}$$

The equations for lift and pitching moment on a pitching wing can be obtained from the equations

$$\frac{C_L'}{\left(\frac{c_o\dot{\theta}}{V_o}\right)} = C_{L_q}' = \frac{2}{Sc_o M_o}\int_{-M_o t}^{c_o - M_o t} m(x+M_o t)^2 P_1\, dx \tag{30}$$

$$\frac{C_m'}{\left(\frac{c_o\dot{\theta}}{V_o}\right)} = C_{m_q}' = -\frac{2}{Sc_o^2 M_o}\int_{-M_o t}^{c_o - M_o t} m(x+M_o t)^3 P_1\, dx \tag{31}$$

where the primes indicate the wing is pitching about and the moments are measured about the leading edge.

A combination of equations (29) and (30) gives for the lift coefficient

for $0 \leq t_o \leq \frac{1}{M_o+1}$ (first interval)

$$C_{L_q}' = \frac{8}{3M_o}\left(1 + \frac{3}{2}t_o^2 - M_o t_o^3\right) \tag{32a}$$

for $\frac{1}{M_o+1} \leq t \leq \frac{1}{M_o-1}$ (second interval)

$$C_{L_q}' = \frac{8}{\pi M_o}\left[\left(\frac{1}{2}t_o^2 - \frac{1}{3}M_o t_o^3 + \frac{1}{3}\right)\arccos\frac{M_o t_o - 1}{t_o} + \frac{M_o}{3\beta}\arccos\left(M_o - \beta^2 t_o\right) + \left(\frac{2}{9}t_o^2 + \frac{1}{9}M_o^2 t_o^2 - \frac{7}{18}M_o t_o + \frac{11}{18}\right)\sqrt{t_o^2 - (1-M_o t_o)^2}\right] \tag{32b}$$

and for $\frac{1}{M_o-1} \leq t_o$ (third interval)

$$C_{L_q}' = 8/3\beta \tag{32c}$$

Similarly a combination of equations (29) and (31) yields, for the pitching moment about the apex, the results

for $0 \leq t_o \leq \frac{1}{M_o+1}$ (first interval)

$$C_{m_q}' = -\frac{2}{M_o}\left[1 + t_o^2 - \frac{1}{8}t_o^4\left(1+4M_o^2\right)\right] \tag{33a}$$

for $\frac{1}{M_o+1} \leq t_o \leq \frac{1}{M_o-1}$ (second interval)

$$C_{m_q}' = -\frac{1}{\pi M_o}\left\{\left[2(1+t_o^2) - \frac{1}{4}t_o^4\left(1+4M_o^2\right)\right]\arccos\frac{M_o t_o - 1}{t_o} + \frac{2M_o}{\pi\beta}\arccos\left(M_o - \beta^2 t_o\right) + \frac{1}{12}\left[42 - 22M_o t_o + (2M_o^2+3)t_o^2 + (2M_o^2+13)M_o t_o^3\right]\sqrt{t_o^2 - (1-M_o t_o)^2}\right\} \tag{33b}$$

and for $\frac{1}{M_o-1} \leq t_o$ (third interval)

$$C_{m_q}' = -\frac{2}{\beta} \tag{33c}$$

Numerical results for a Mach number of 2 are presented in the next section.

## Discussion of Results

Figure 4 shows the variation of $C_{L_\alpha}$, $C_{m_\alpha}'$, and the location of $x_{c.p.}$ with $\tau_o$, the number of chord lengths traveled ( $\tau_o = V_o t'/c_o = M_o t/c_o = M_o t_o$) for a free-stream Mach number $M_o$ equal to 2. The values of $C_{L_\alpha}$ and $C_{m_\alpha}'$ are in agreement with those given in references 1 and 2. For the purpose of comparison, similar curves are shown for a two-dimensional wing having a chord $c_o$ equal to the root chord of the triangular wing, and for the triangular wing in reversed flow. The material necessary for the calculation of the latter curves was presented in reference 6. Several interesting conclusions can be drawn from these results.

First, notice that the total indicial lift on the triangular sinking wing is the same at every instant as that on the same wing in reversed flow (both wings of course having started with the same velocity at the same time), and that the value of this lift is the same as the total indicial lift on the two-dimensional wing only at the beginning of the motion and again when the steady state has been attained (fig. 4(a)). Such a result for reversed flow is not true for the pitching moment (fig. 4(b)) and center of pressure, and it can be shown that it is true for the total lift only when the wing is a flat lifting surface with supersonic edges.[4]

Second, notice that, since all of the characteristics for the triangular wings are independent of the angle of sweep, they are valid for any unyawed triangular wing flying at a Mach number equal to 2 and having supersonic leading edges.

Third, it is apparent from figure 4(a) that the transition of the total indicial lift from its initial to its final value is less abrupt than that transition for the two-dimensional wing, and finally the movement of the center of pressure on the sinking wing of all types is seen from figure 4(c) to be small.

[4] R. T. Jones has shown, in an unpublished work, that the build-up of total indicial drag on symmetrical nonlifting wings is the same for all types of plan forms in forward and reversed flow.

Finally, it can be seen from equations (27a) and (27c) that the initial and final values of $C_{L_\alpha}$ depend on $1/M_o$ and $1/\beta$, respectively. As the Mach number $M_o$ is increased, therefore, the variation dies out since $\beta$ and $M_o$ become nearly equal. The same remark applies to all the other coefficients.

Figure 5 presents the values of $C_{L_q}'$, $C_{m_q}'$, and $x_{c.p.}/c_o$ for wings pitching about the foremost extremity of their plan form (i.e., leading edge or apex). Again the results are presented in terms of chord lengths traveled $\tau_o$ for a free-stream Mach number equal to 2.

For these wings it is apparent that the reverse-flow theorem does not apply even to total lift. The results for the triangular wing are still independent of the angle of sweep, however, and the movement of the center of pressure is again slight.

## W I N G  W I T H  S U B S O N I C  E D G E S

### INDICIAL LOADING FOR SINKING WING

#### Analysis

The six regions.- As in the study of supersonic-edged triangular wings, there are also in the case of triangular wings with subsonic leading edges various regions in which the analytical form of the loading equation is different. Figure 6 shows the regions into which the subsonic-edged triangular wing can be most conveniently divided. Most of these regions have counterparts on the supersonic-edged wing shown in figure 1.

To begin with, region 6 lies within the spherical wave which started at $t=0$ from the wing apex. Region 1 is within the cylindrical wave which was started at $t=0$ by one edge of the wing, but outside the wave started by the other edge. Region 4 is the area formed by the overlapping of the two cylindrical waves from the opposite edges, but outside the region influenced by the reflection of one of these waves on the opposite edge (secondary wave fronts shown in the figure). Region 5 is the area between regions 4 and 6 where the flow is influenced by secondary (and higher-order) wave reflections. Finally, regions 2 and 3 are similar to regions 2 and 3 in the supersonic-edged case; region 2 being that uninfluenced by the starting phenomena and therefore having a loading already at its steady-state value, and region 3 being that which is unaffected by the disturbances emanating from the edges.

Region 1: The solution for the load distribution in region 1 is the same as that for a two-dimensional wing starting suddenly from rest and moving with a steady subsonic velocity $V_n$. A solution to the latter problem for the initial part of the motion is presented in reference 7. In terms of the normal components of velocity and distance, therefore, the loading coefficient for the right-hand side of figure 6 can be written immediately:

$$\left(\frac{\Delta p}{q_n}\right)_1 = -\frac{8w_o}{\pi V_n M_n}\left(\frac{M_n}{1+M_n}\sqrt{\frac{t-x_n}{M_n t+x_n}} + \arctan\sqrt{\frac{M_n t+x_n}{t-x_n}}\right)$$

The equations which relate the normal components to those in the free-stream direction have already been given in the section on region 4 of the supersonic-edged wing. Use of these relations leads to the following expression for loading in region 1 (in the coordinate system of fig. 7)

$$\left(\frac{\Delta p}{q_o}\right)_1 = \frac{8\alpha}{\pi M_o}\left(\frac{mM_o}{mM_o+\sqrt{1+m^2}}\sqrt{\frac{t\sqrt{1+m^2}+|y|-mx}{m\,M_o t-|y|+mx}} + \arctan\sqrt{\frac{mM_o t-|y|+mx}{t\sqrt{1+m^2}+|y|-mx}}\right) \tag{34}$$

Region 2: The loading on region 2, being the steady-state loading on a triangular wing with subsonic edges, is well known. The solution for region 2 of figure 7 is therefore given by (see, for convenience, reference 5)

$$\left(\frac{\Delta p}{q_o}\right)_2 = \frac{4\alpha m^2(x+M_o t)}{\sqrt{m^2(x+M_o t)^2-y^2}}\,E \tag{35}$$

where $E$ is the complete elliptic integral of the second kind with modulus $\sqrt{1-\beta^2 m^2}$

Region 3: The loading in region 3 follows from reference 6 and is

$$\left(\frac{\Delta p}{q_o}\right)_3 = \frac{4\alpha}{M_o} \tag{36}$$

Region 4: The loading in region 4 of figure 7 is calculated by superposition, just as the solution for region 5 of the wing with supersonic edges was obtained. The solution in region 4 is the sum of the solutions for the right and left halves of region 1, minus the result for region 3. Thus

$$\left(\frac{\Delta p}{q_o}\right)_4 = \frac{8\alpha}{\pi M_o}\left[\frac{mM_o}{mM_o+\sqrt{1+m^2}}\left(\sqrt{\frac{t\sqrt{1+m^2}-y-mx}{mM_o t+y+mx}}+\sqrt{\frac{t\sqrt{1+m^2}+y-mx}{mM_o t-y+mx}}\right)+\arctan\sqrt{\frac{mM_o t+y+mx}{t\sqrt{1+m^2}-y-mx}}+\arctan\sqrt{\frac{mM_o t-y+mx}{t\sqrt{1+m^2}+y-mx}}-\frac{\pi}{2}\right] \tag{37}$$

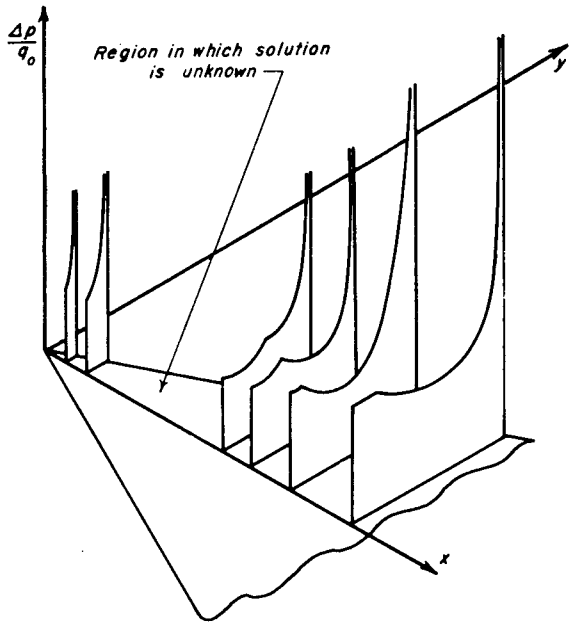


Regions 5 and 6: In these regions the exact solution for the loading has not been determined. As was shown in reference 4, such solutions would require the solution of a three-dimensional elliptic-type partial differential equation. In this report a later section will contain an approximate solution for these regions.

## Discussion of Results

An isometric drawing of the load distribution, for the regions in which it is known, is shown in the sketch. Comparing the results for the loading on this wing to the one with supersonic edges (fig. 3), it is apparent that the principal difference in the two distributions is in the behavior around the leading edges; the loading being finite at the supersonic edge, whereas it becomes infinite at the subsonic edge. In view of the known steady-state results this difference was to be expected. Elsewhere the loadings are quite similar.

The results presented in equations (34) through (37) will next be examined in a different light. Choose a given spanwise section on the wing and watch this section as time progresses from t=0. This amounts to fixing the axis on the body and can be accomplished simply by using the quantity s introduced in equation (21),

$$s = m(x + M_o t)$$

It is clear that s is the semispan of a given spanwise section, and that if equations (34) through (37) are written in terms of s, y, and t, for a fixed s they represent the variation of loading on a given section as time progresses.

If the notation is further simplified by introducing the parameter $\beta_e$ where

$$\beta_e = \frac{1}{mM_o + \sqrt{1+m^2}} \tag{38}$$

equations (34) through (37) can be written in the following way:

$$\left(\frac{\Delta p}{q_o}\right)_1 = \frac{8\alpha}{\pi M_o}\left(mM_o\beta_e\sqrt{\frac{t/\beta_e - s + |y|}{s - |y|}} + \arctan\sqrt{\frac{s - |y|}{t/\beta_e - s + |y|}}\right) \tag{39}$$

$$\left(\frac{\Delta p}{q_o}\right)_2 = \frac{4\alpha ms}{E\sqrt{s^2 - y^2}} \tag{40}$$

$$\left(\frac{\Delta p}{q_o}\right)_3 = \frac{4\alpha}{M_o} \tag{41}$$

$$\left(\frac{\Delta p}{q_o}\right)_4 = \frac{8\alpha}{\pi M_o}\left(mM_o\beta_e\sqrt{\frac{t/\beta_e + y - s}{s - y}} + mM_o\beta_e\sqrt{\frac{t/\beta_e - y - s}{s + y}} + \arctan\sqrt{\frac{s - y}{t/\beta_e + y - s}} + \arctan\sqrt{\frac{s + y}{t/\beta_e - y - s}} - \frac{\pi}{2}\right) \tag{42}$$

The load distribution across any section is given by equations (39), (41), and (42) from the time $t/\beta_e = 0$ to $(t/\beta_e)_1$, where the term $(t/\beta_e)_1$ is equal to $2s$ or $s/m(M_o+1)\beta_e$, whichever is smaller.

(At $t/\beta_e = 2s$ the spanwise section has just reached the secondary waves shown in figure 6, and at $t/\beta_e = s/m\beta_e(M_o+1)$ the spanwise section has just reached the spherical wave which started from the apex.) From $(t/\beta_e)_1$ to $(t/\beta_e)_2 = s/m\beta_e(M_o-1)$, the loading has not been determined, and from $t/\beta_e = (t/\beta_e)_2$ to $t=\infty$ the loading is the steady-state value given by equation (40). The sketch shows this initial and final load variation plotted as a function of the parameter $t/\beta_e$. At the beginning of the motion the loading is constant across the span, but this type of distribution is quickly modified and the shape of the curve tends toward the "inverted elliptic" loading given by equation (40) and shown in the sketch as the distribution at $t/\beta_e = (t/\beta_e)_2$. In fact, when the span has traveled a distance such that $t/\beta_e=2s$, the expression for the loading given by equation (42) becomes

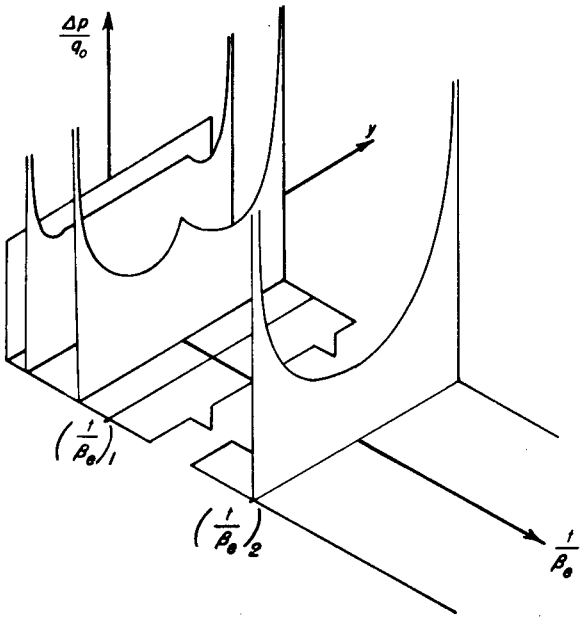


$$\left(\frac{\Delta p}{q_o}\right)_{\frac{t}{\beta_e}=2s} = \frac{16\, m\beta_e s}{\pi\sqrt{s^2-y^2}} \qquad (43)$$

which differs from the value given by equation (40) only by a constant of proportionality. Both before and after the time $t/\beta_e=2s$ the shape of the loading curve varies from the simple type represented by equation (43), but the trend, and to a certain extent the rapidity of the trend, is clearly established.

The average spanwise loading $P_o$, introduced by equation (20a), can now be determined for certain regions. Hence, if the notation

$$\left.\begin{aligned} \tau &= t/s \\ P_o &= \frac{M_o}{2s\alpha}\int_{-s}^{s}\frac{\Delta p}{q_o}\,dy \end{aligned}\right\} \qquad (44)$$

is adopted, there results for the early part of the motion, that is, for $0 \le \tau/\beta_e \le (\tau/\beta_e)_1$,

$$P_o = 2\left(2 - \frac{\tau}{\beta_e}\right) + 4m\beta_e M_o\,(\tau/\beta_e) \qquad (45)$$

Equation (45) was derived by integrating equations (39), (41), and (42). For values of $\tau/\beta_e \geq 1/\beta_e m(M_o-1) = \left(\frac{\tau}{\beta_e}\right)_2$ equation (40) is valid. Hence

for $\frac{\tau}{\beta_e} \geq \left(\frac{\tau}{\beta_e}\right)_2$

$$P_o = \frac{2\pi m M_o}{E} \tag{46}$$

The sketch indicates the magnitude of this average load for both large and small values of $\tau/\beta_e$. Notice that for small values of $\tau/\beta_e$ it is sufficient for the establishment of the curve to specify the parameter $mM_o\beta_e$, but for large values an additional parameter must be given (such as $M_o$ in the sketch). Notice, further, that in spite of the large variation in the distribution of the loading, as shown in the previous sketch, the average value $P_o$ varies linearly throughout the intervals considered. This result is similar to the one obtained for triangular wings with supersonic edges and is given in equations (24).

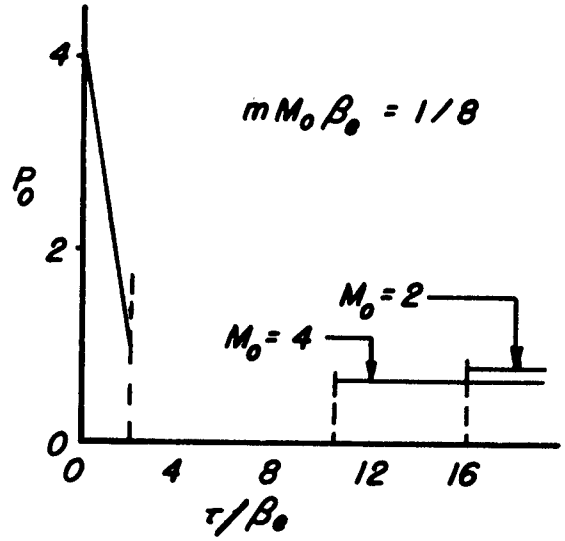


## INDICIAL LOADING ON VERY SLENDER TRIANGULAR WINGS

### Analysis

In the first section of this report entitled "The Problem and the Nature of its Solution," it was pointed out that if the wing is slender (i.e., has a small ratio of span to chordwise length) the basic partial differential equation (1) can be approximated by the equation which was previously introduced as equation (4), thus:

$$\varphi_{tt} - \varphi_{yy} - \varphi_{zz} = 0$$

The boundary conditions appropriate to this problem will now be examined in some detail.

Just as in the previous sections of this report, consider a triangular wing which is at rest for $t < 0$, starts suddenly to move at a forward velocity equal to $V_o$ at $t=0$, and continues at this same velocity for $t > 0$. It should be emphasized that in this case, $V_o$ may be either subsonic or supersonic. A section in the spanwise direction, as for instance section AA in the sketch, projects into the $yt$ plane as a narrow rectangular strip along the $t$ axis. Since equation (4) has been derived on the assumption that the velocity gradients in the $y$, $z$, and $t$ directions are independent of the gradient in the $x$ direction, the boundary conditions along the strip shown in the sketch are independent of those on other strips projected from spanwise sections along the wing. Hence, the problem is to find a solution to equation (4) which will make $\varphi_z$ constant over the strip and at the same time will satisfy the other conditions listed under equation (1). In the lifting-surface analog this corresponds to the problem of finding the velocity potential over a flat rectangular wing of low aspect ratio situated in a free stream moving at a Mach number equal to $\sqrt{2}$. Solutions to the latter problem can be obtained by various techniques, and so the procedure will be first, to find the potential for the steady-state, flat, rectangular wing, and then, by analogy, to convert this to the solution for the very slender triangular wing in unsteady motion.

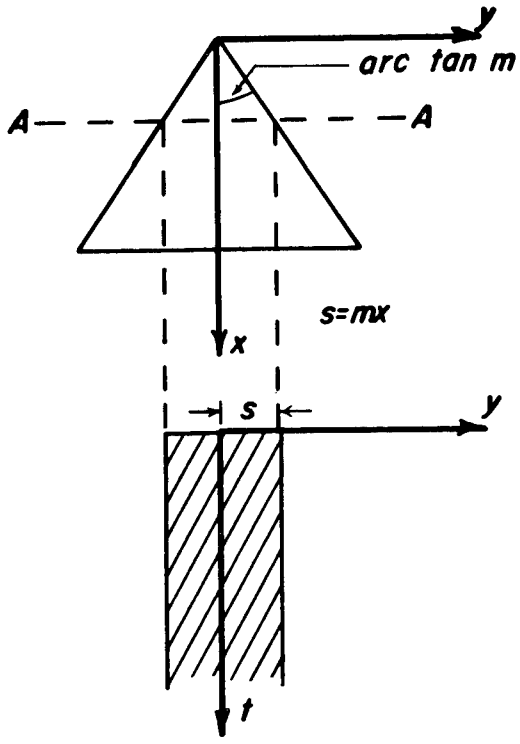


The steady-state, lifting-surface problem.- Lifting-surface solutions for the loading on a rectangular wing traveling at supersonic speeds have been developed for regions 1, 2, and 3 of figure 8 (by Busemann and others), and by means of these solutions the load distribution on a spanwise section of the triangular wing can be determined to a time necessary for sound to travel that span length. For $t > 2s$, however, the solution becomes considerably complicated by the increasing number of reflections from the edges. Reference 8 gives solutions for the loading on a rectangular wing in region 4 and indicates methods for extending the solution to regions farther along the wing. Already in region 4, however, the expression is cumbersome and in higher-numbered regions the expressions become difficult to manipulate. These methods, therefore, will be discarded in favor of a more approximate but simpler analysis.

If $x$ is the distance along the chord, $y$ the distance along the span, and $s$ the semispan, then the solution for regions 1, 2, and 3 of

figure 8 can be written (for convenience, see reference 5):

Region 1

$$\frac{\Delta p}{q_o} = 4\alpha \tag{47a}$$

Region 2

$$\frac{\Delta p}{q_o} = \frac{8\alpha}{\pi} \arctan \sqrt{\frac{s - |y|}{x - s + |y|}} \tag{47b}$$

Region 3

$$\frac{\Delta p}{q_o} = \frac{8\alpha}{\pi} \left( \arctan \sqrt{\frac{s+y}{x-s-y}} + \arctan \sqrt{\frac{s-y}{x-s+y}} - \frac{\pi}{2} \right) \tag{47c}$$

As x increases (i.e., for higher-numbered regions in figure 8) it is reasonable to assume that the spanwise variation of loading is relatively unimportant – except that it be "smooth" and fall to zero at the side edges – and the chordwise variation of loading is dominant. Assume, therefore, that the loading is given by the relation

$$\frac{\Delta p}{q_o} = 4\alpha f\left(\frac{x}{s}\right) \sqrt{1 - \left(\frac{y}{s}\right)^2} \tag{48}$$

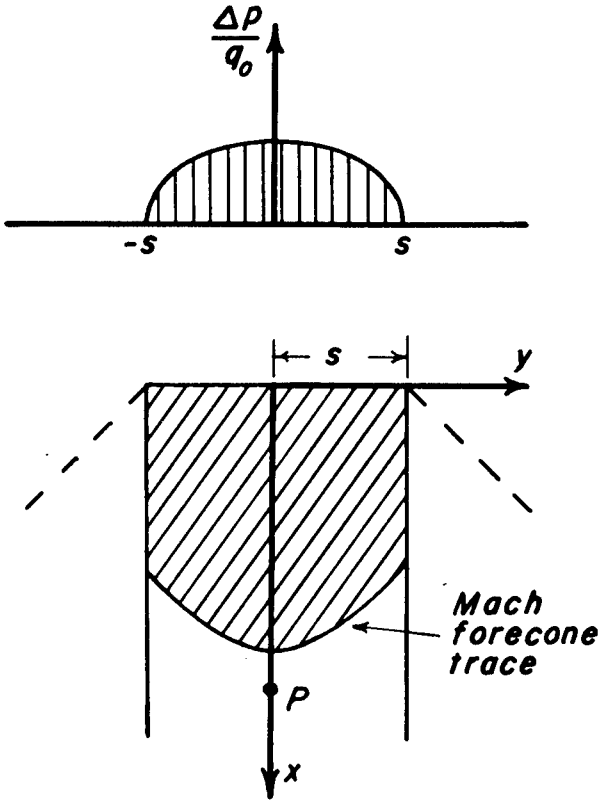

Spanwise, this has the variation shown in the preceding sketch; chordwise it is as yet arbitrary. To fix the chordwise distribution the value of $f(x/s)$ will be determined so that the vertical induced velocity along the center line is constant and equal to $-V_o\alpha$.

The solution to this somewhat artificial problem approaches the exact solution to the steady-state lifting-surface problem for a flat rectangular wing along sections far behind the leading edge; closer to the leading edge it only approximates the exact solution; and, of course, in the vicinity of the leading edge it will be least representative. But, on the other hand, the exact solution is known in the vicinity of the leading edge and it turns out that the solution of the problem posed above forms a reasonable continuation over the remainder of the wing.

The velocity potential for the problem which has been set can be readily expressed in terms of an integration of elementary horseshoe vortices over the plan form. Since the Mach number equals $\sqrt{2}$, then according to reference 9,

$$\varphi = \frac{V_o z}{4\pi} \int_A \int \frac{(x-x_1)\ (\Delta p/q_o)\ dx_1 dy_1}{(y_1^2+z^2)\ \sqrt{(x-x_1)^2 - y_1^2 - z^2}}$$

where $A$ is the area on the wing within the forecone from the point $P(x,y,z)$, at which $\varphi$ is to be determined (the shaded area in the sketch).

The simplification of the last expression is given in reference 9. The result is the integral equation

$$1 = f(\eta) + \frac{2}{\pi} \int_o^{\eta} f(\eta_1)\ G\ (\eta-\eta_1) d\eta_1 \qquad (49)$$

where $\eta=x/s$ and $G$ is given by

$$G(\eta-\eta_1) = \begin{cases} E_1 & 1 \leq \eta-\eta_1 \\ \dfrac{E_2-(1-k_2^2)K_2}{k_2} & \eta-\eta_1 \leq 1 \end{cases}$$

$$k_1 = \frac{1}{\eta-\eta_1}\ ;\quad k_2 = \eta-\eta_1$$

The modulus of $E_1$ is $k_1$ and the modulus of $K_2$ and $E_2$ is $k_2$.

The solution of equation (49) for $f(\eta)$ is not difficult when numerical methods are used. For intervals of $\eta_1$ equal to 0.2, the result is given in tabular form in appendix A, and also in the sketch.

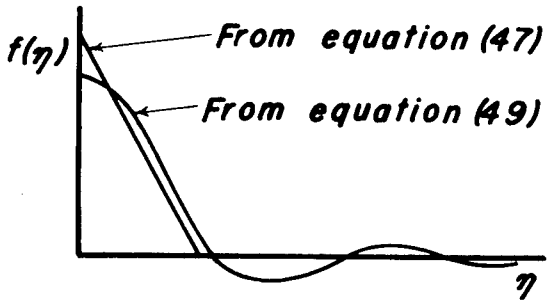


This result can be improved in the interval $0 \leq \eta \leq 2$ by means of the correct solution in that interval given by equations (47). Comparison of the spanwise average of the loading given by equation (48) with that which can be derived from equations (47) gives an equivalent $f(\eta)$ in the interval which, when used in equation (48), will give the correct value of the average span loading. The sketch also shows a curve for this equivalent $f(\eta)$ which starts at $4/\pi$ and falls linearly to zero at $\eta=2$.

By using the sketch, or the results listed in appendix A, the loading over a low-aspect-ratio rectangular wing flying at a Mach number equal to $\sqrt{2}$ can be estimated. Of particular interest is the damped oscillatory nature of the load, falling to zero at one span length behind the leading edge and taking alternately negative and positive values beyond this point.[5] A somewhat different approach to this problem (reference 11) has recently led to a solution very like the one given here.

The unsteady analog, sinking wing.- The first step in deriving the unsteady-flow results for the sinking wing from the steady solution is to replace $x$ with $t$. In equation (49) this corresponds to replacing $\eta$ with $\tau$ where $\tau$ is equal to $t/s$ (equation (44). The second step is to rederive the expression for loading coefficient since in the time-varying problem it is expressed in a somewhat different manner than in the steady-state analog. In the unsteady case, as the triangular wing moves through a fixed reference plane the local span intersecting

[5] A discussion of this aspect of these results is contained in reference 10.

this plane grows as a function of time and equation (2), which represents the partial derivative with respect to time with x fixed, must be expanded to the form

$$\frac{\Delta p}{q_o} = \frac{2}{V_o M_o}\left[\frac{\partial \Delta\varphi}{\partial t}\right]_x = \frac{2}{V_o M_o}\left(\left[\frac{\partial \Delta\varphi}{\partial t}\right]_s + \left[\frac{\partial \Delta\varphi}{\partial s}\right]_t \frac{\partial s}{\partial t}\right)$$

where $\left[\frac{\partial \Delta\varphi}{\partial t}\right]_s$ and $\left[\frac{\partial \Delta\varphi}{\partial s}\right]_t$ indicate derivatives taken at constant s and t, respectively. Since s is equal to $m(x + M_o t)$, $\partial s/\partial t$ equals $mM_o$, and there results

$$\frac{\Delta p}{q_o} = \frac{2}{V_o M_o}\left(\left[\frac{\partial \Delta\varphi}{\partial t}\right]_s + mM_o \left[\frac{\partial \Delta\varphi}{\partial s}\right]_t\right) \tag{50}$$

In the steady-state problems an analog to the term involving $\left[\frac{\partial \Delta\varphi}{\partial s}\right]_t$ is missing, and the loading coefficient is given entirely by an operation equivalent to $\left[\frac{\partial \Delta\varphi}{\partial t}\right]_s$. It is necessary, therefore, to operate further on the solution given for the loading in the steady-state problem to obtain the solution for the loading in the unsteady problem. But

$$\left[\frac{\partial \Delta\varphi}{\partial s}\right]_t = \frac{\partial}{\partial s}\int_o^t \left[\frac{\partial \Delta\varphi}{\partial t}\right]_s dt_1$$

so that if the notation

$$\left[\frac{\partial \Delta\varphi}{\partial t}\right]_s = \frac{V_o}{2}\left(\frac{\Delta p}{q_o}\right)_s$$

is adopted (where $\left(\frac{\Delta p}{q_o}\right)_s$ represents the loading in the analogous steady-state problem), then the expression for the unsteady loading can be given in terms of $\left(\frac{\Delta p}{q_o}\right)_s$ by the equation

$$\frac{\Delta p}{q_o} = \frac{1}{M_o}\left[\left(\frac{\Delta p}{q_o}\right)_s + mM_o \frac{\partial}{\partial s}\int_o^t \left(\frac{\Delta p}{q_o}\right)_s dt_1\right] \tag{51}$$

By the application of equation (51) to equations (47), the loading for the various regions of the unsteady wing can be found. For region 2 there results

$$\frac{\Delta p}{q_o} = \frac{1}{M_o}\left[\frac{8\alpha}{\pi}\arctan\sqrt{\frac{s-|y|}{t-s+|y|}} + mM_o\frac{\partial}{\partial s}\left(\int_o^{s-|y|} 4\alpha\, dt_1 + \right.\right.$$

$$\left.\left.\int_{s-|y|}^{t}\frac{8\alpha}{\pi}\arctan\sqrt{\frac{s-|y|}{t_1-s+|y|}}\,dt_1\right)\right]$$

which becomes

$$\frac{\Delta p}{q_o} = \frac{8\alpha}{\pi M_o}\left[mM_o\sqrt{\frac{t-s+|y|}{s-|y|}} + \arctan\sqrt{\frac{s-|y|}{t-s+|y|}}\right]$$

The loading coefficient can be similarly derived in the other regions so that finally

Region 1

$$\frac{\Delta p}{q_o} = \frac{4\alpha}{M_o} \tag{52a}$$

Region 2

$$\frac{\Delta p}{q_o} = \frac{8\alpha}{\pi M_o}\left(mM_o\sqrt{\frac{t-s+|y|}{s-|y|}} + \arctan\sqrt{\frac{s-|y|}{t-s+|y|}}\right) \tag{52b}$$

Region 3

$$\frac{\Delta p}{q_o} = \frac{8\alpha}{\pi M_o}\left(mM_o\sqrt{\frac{t-s+y}{s-y}} + mM_o\sqrt{\frac{t-s-y}{s+y}} + \right.$$

$$\left.\arctan\sqrt{\frac{s-y}{t-s+y}} + \arctan\sqrt{\frac{s+y}{t-s-y}} - \frac{\pi}{2}\right) \tag{52c}$$

For the interval $t \geq 2s$ equation (48) must be considered. By means of equation (51), the expression for the loading coefficient can be written

$$\frac{\Delta p}{q_o} = \frac{1}{M_o}\left[4\alpha\, f(\tau)\sqrt{1-\left(\frac{y}{s}\right)^2} + mM_o\frac{\partial}{\partial s}\int_o^t 4\alpha\, f\left(\frac{t_1}{s}\right)\sqrt{1-\left(\frac{y}{s}\right)^2}\, dt_1\right]$$

which becomes

$$\frac{\Delta p}{q_o} = \frac{4\alpha}{M_o}\left[(1-mM_o\tau)\sqrt{1-\left(\frac{y}{s}\right)^2}\, f(\tau) + \frac{mM_o}{\sqrt{1-\left(\frac{y}{s}\right)^2}}\int_o^\tau f(\tau_1)d\tau_1\right] \qquad (53)$$

where $f(\tau)$ is the solution to equation (49). Notice that for large $\tau$ (when the loading has reached its steady state), $f(\tau)$ is zero and $\int_o^\tau f(\tau_1)d\tau_1$ is unity. (See appendix A.) Hence, the loading is given by the equation

$$\frac{\Delta p}{q_o} = \frac{4\alpha ms}{\sqrt{s^2-y^2}}$$

which is the steady-state value for a slender triangular wing (equation (40) when $E = 1$).

It is now possible to derive the average span loading $P_o$ as defined by equation (20a), thus

$$P_o = \frac{M_o}{2s\alpha}\int_{-s}^{s}\frac{\Delta p}{q_o}\, dy$$

Placing equations (52) and (53) in this expression, it is found that

for $0 \leq \tau \leq 2$

$$P_o = 2(2-\tau) + 4mM_o\tau \qquad (54a)$$

and for $\tau \geq 2$

$$P_o = \pi(1-mM_o\tau)f(\tau) + 2\, mM_o\pi\int_o^\tau f(\tau_1)\, d\tau_1 \qquad (54b)$$

Since the values of $P_o$ given by equations (54a) and (54b) were derived using different methods, their magnitudes at $\tau = 2$ are not

equal. The final curve for $P_o$ must be constructed by fairing the solution for $\tau \leq 2$ into that for $\tau > 2$. The accompanying sketch shows these results together with the final curve chosen (solid line).

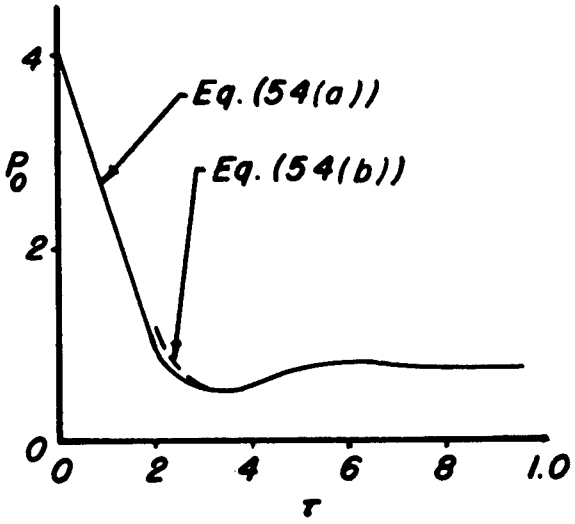


The unsteady analog, pitching wing.— When the wing is pitching at a steady rate about its apex, the equation for the vertical induced velocity on the plan form is

$$w_u = -(x + M_o t)\dot{\theta}$$

so that the $\alpha$ in the steady-state equations (47) and (48) must be replaced by $\dot{\theta}s/mV_o$. Since the loading coefficient is still given by equation (51), there results for the conversion of equation (48) the expression

$$\frac{\Delta p}{q_o} = \frac{4\dot{\theta}}{mM_oV_o}\left[\sqrt{s^2-y^2}\, f(\tau) + mM_o \frac{\partial}{\partial s} s\sqrt{s^2-y^2} \int_o^{t/s} f(\tau_1)\, d\tau_1\right]$$

and this can be reduced to the form

$$\frac{\Delta p}{q_o} = \frac{4\dot{\theta}}{mM_oV_o} (1-mM_o\tau) \sqrt{s^2-y^2}\, f(\tau) +$$

$$\frac{4\dot{\theta}}{V_o} \left(\frac{2s^2-y^2}{\sqrt{s^2-y^2}}\right) \int_o^\tau f(\tau_1)\, d\tau_1 \qquad (55)$$

As in the discussion of equation (53), it can be seen that equation (55) becomes for the steady state ($\tau$ large)

$$\frac{\Delta p}{q_o} = \frac{4\dot{\theta}}{V_o} \left(\frac{2s^2-y^2}{\sqrt{s^2-y^2}}\right)$$

and this can be shown to agree with the steady-state slender-wing results given in reference 12.

It is now possible to derive the average span loading $P_1$ as defined by equation (20b)

$$P_1 = \frac{mM_oV_o}{2s^2\dot{\theta}} \int_{-s}^{s} \frac{\Delta p}{q_o}\, dy$$

Using equation (55), one finds for $\tau > 2$

$$P_1 = \pi(1-mM_o\tau)\, f(\tau) + 3mM_o\pi \int_o^\tau f(\tau_1)\, d\tau_1 \qquad (56a)$$

and a similar analysis based on equation (47) yields

for $0 \leq \tau \leq 2$

$$P_1 = \frac{2s}{m} \left(2-\tau+4mM_o\tau-\frac{1}{2}\, mM_o\tau^2\right) \qquad (56b)$$

As in the case for $P_o$, the two equations for $P_1$ do not join at $\tau=2$ and the final curve must be constructed by fairing the solution for $\tau \leq 2$ into that for $\tau \geq 2$.

Discussion of Results

It is now possible to assess the accuracy of the solution for very slender wings in the interval $0 \leq \tau \leq 2$ by comparing equations (52) and (54a) with equations (41), (39), (42), and (45), the exact solutions for this region derived in the preceding section. It is apparent that the approximate solution differs from the exact only by a stretching factor in the t direction. Hence, if $\tau$ is replaced by $\tau/\beta_e$ and m (note m is proportional to y/t) by $m\beta_e$, where $\beta_e$ is given by equation (38), then equations (52a), (b), and (c) are identical with equations (41), (39), and (42), respectively, and, of course, equation (54a) corresponds to equation (45).

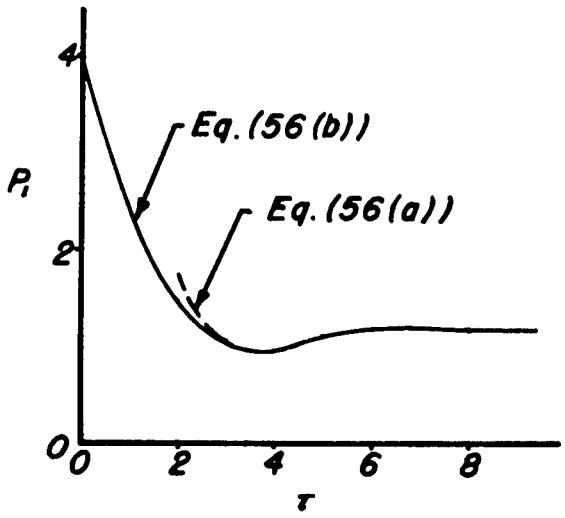


This rather remarkable result can be enlarged upon from another viewpoint. Suppose that in the steady-state analog problem the wing had been flying at some Mach number other than $\sqrt{2}$, say $M_e$. The solution to such a new problem could be obtained from the old one merely by applying the Prandtl-Glauert correction, that is, by stretching all distances in the x direction by the factor $1/\beta_e$ where $\beta_e^2 = |1-M_e^2|$. Such a procedure would convert, for example, equation (54a) to the form

$$P_o\beta_e = 2(2-\tau/\beta_e) + 4m\beta_e M_o \tau/\beta_e$$

Finally, if $P_o$ is adjusted so that $P_o=4$ at $\tau=0$, there results

$$P_o = 2(2-\tau/\beta_e) + 4mM_o\tau$$

which is exactly the answer given by equation (45). It is possible to simplify the statement of this procedure by simply remarking: The exact results for $\Delta p/q_o$ or $P_o$ in the interval $0 \leq \tau/\beta_e \leq 2$ can be obtained from the approximate results for a very slender wing by making an effective Mach number correction to the right-hand side of equations (52) or (54a), respectively.

It is interesting to pursue this concept even further. Consider a spanwise section of a triangular wing as time increases from the starting impulse. The primary wave fronts emanating from either side pass across the section forming the Mach lines in the steady-state rectangular-wing analogy. For very slender wings these lines make a $45^\circ$ angle with the trace of the side edge and are used to divide the plan form into regions as in the sketch. Now find the actual position of these primary wave fronts as they form a trace on the section in the $y\tau$ plane. A straightforward calculation shows that these lines actually make an angle equal to arc tan $1/\beta_e$ with the trace of the side edges. Hence the effective Mach number which is used to correct the slender-wing results in the interval $0 \leq \tau \leq 2\beta_e$ is that which makes the Mach lines of the steady-state analogy coincide with the actual trace of the primary wave fronts.

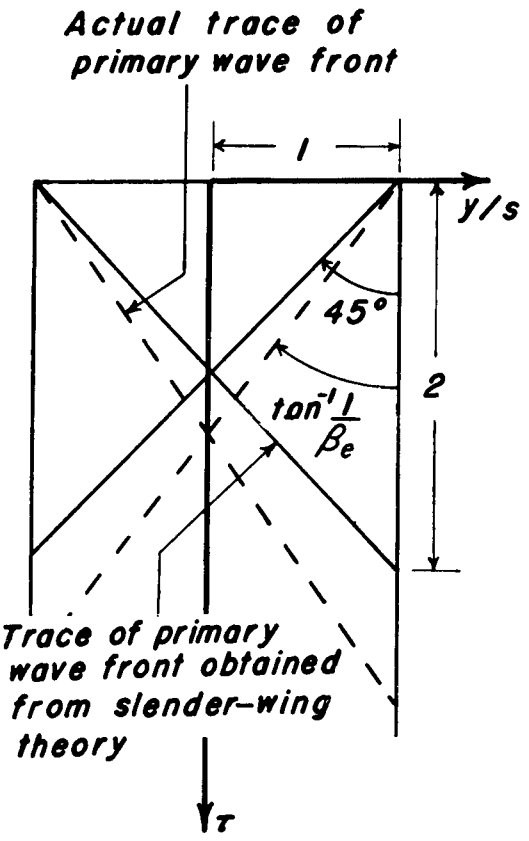


## INDICIAL LIFT AND PITCHING MOMENT ON VERY SLENDER TRIANGULAR WINGS

### Analysis

The lift coefficient for the sinking wing is given in the notation introduced in equation (21a) by the equation

$$C_L = \frac{\alpha}{mc_o^2} \int_o^{c_o} \frac{2s}{M_o} P_o dx$$

where $P_o$ has been determined in the last section as a function of $\tau=t/s$. Consider the situation at a certain fixed time and let the $x$ coordinate in the above formula be fixed in the wing. Then set

$$\zeta = \frac{x}{c_o} = \frac{s}{mc_o} \tag{57}$$

and as before

$$\tau_o = \frac{M_o t}{c_o} = mM_o \zeta \tau \tag{58}$$

where $\tau_o$ is the number of wing-chord lengths traveled. In this way the equation for lift coefficient becomes

$$M_o C_{L_\alpha} = 2 \int_o^1 \zeta \, P_o \left( \frac{\tau_o}{mM_o \zeta} \right) d\zeta \tag{59}$$

and by a similar analysis the pitching-moment coefficient taken about the apex can be written

$$M_o C_{m_\alpha}{}' = -2 \int_o^1 \zeta^2 \, P_o \left( \frac{\tau_o}{mM_o \zeta} \right) d\zeta \tag{60}$$

The equation for the lift and pitching-moment coefficients (where again the pitching moment is taken about the apex) on a pitching wing are

$$M_o C_{L_q}{}' = \frac{M_o C_L}{\left( \frac{c_o \dot{\theta}}{V_o} \right)} = 2 \int_o^1 \zeta^2 \, P_1 \left( \frac{\tau_o}{mM_o \zeta} \right) d\zeta \tag{61}$$

and

$$M_o C_{m_q}{}' = \frac{M_o C_m}{\left( \frac{c_o \dot{\theta}}{V_o} \right)} = -2 \int_o^1 \zeta^3 \, P_1 \left( \frac{\tau_o}{mM_o \zeta} \right) d\zeta \tag{62}$$

## Discussion of Results

The values of $P_o$ and $P_1$ were taken from curves similar to the sketches in the last section (using the faired curves in the vicinity of $\tau=2$) and the results for the indicial lift and pitching moment in terms of $\tau_o$, the number of chord lengths traveled, are shown in figures (9) and (10) for a value of $mM_o$ equal to 1/8. The results are all

qualitatively alike; in each case the curve falls from its high initial value at $\tau_o=0$ to a minimum at about $\tau_o=1/3$ and then recovers and practically attains its asymptotic value at $\tau_o=1$. This behavior is similar to that for a two-dimensional wing flying at subsonic speeds. For the purpose of such a comparison the first part of the curve of indicial lift coefficient versus chord lengths traveled on a two-dimensional wing flying at a Mach number equal to 0.8 (see reference 7) is shown in the sketch. Notice again the rapid fall from the initial peak ($C_{L_\alpha}=4/M_o$) to a minimum around $\tau_o=1/2$, and then a smooth recovery to the asymptotic value ($C_{L_\alpha}=2\pi/\beta$).

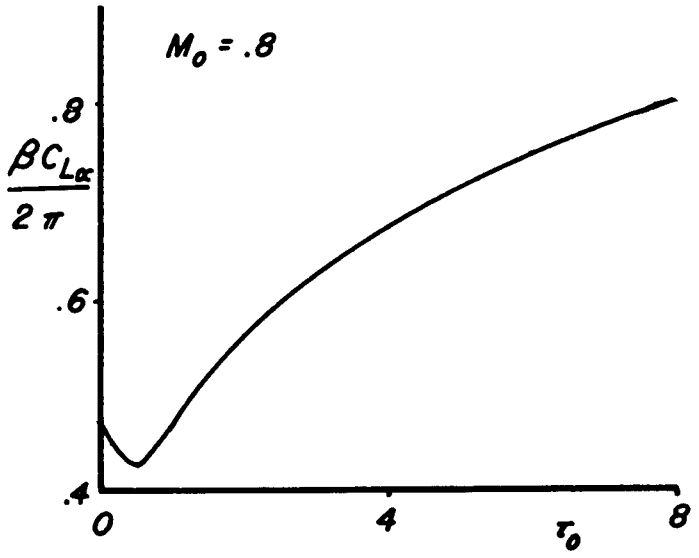


Ames Aeronautical Laboratory,
National Advisory Committee for Aeronautics,
Moffett Field, Calif., Mar. 26, 1951.

## APPENDIX A

## SOLUTION OF AN INTEGRAL EQUATION

For convenience in applying equations (54b) and (56a) of the text, a table of values of the function $f(\eta)$, obtained by numerical solution of equation (49), is given here. The values of the integral, $\int_0^\eta f(\eta_1)d\eta_1$, are also listed.

| $\eta$ | $f(\eta)$ | $\int_0^\eta f(\eta_1)d\eta_1$ | $\eta$ | $f(\eta)$ | $\int_0^\eta f(\eta_1)d\eta_1$ |
|---|---|---|---|---|---|
| 0.0 | 1.0000 | 0.0000 | 4.0 | -0.1307 | 1.0124 |
| .2 | .9899 | .1990 | 4.2 | −.1008 | .9893 |
| .4 | .9597 | .3940 | 4.4 | −.0716 | .9720 |
| .6 | .9087 | .5808 | 4.6 | −.0446 | .9604 |
| .8 | .8356 | .7552 | 4.8 | −.0207 | .9539 |
| 1.0 | .7339 | .9122 | 5.0 | −.0008 | .9517 |
| 1.2 | .6032 | 1.0459 | 5.2 | .0149 | .9531 |
| 1.4 | .4597 | 1.1522 | 5.4 | .0265 | .9573 |
| 1.6 | .3188 | 1.2300 | 5.6 | .0340 | .9633 |
| 1.8 | .1880 | 1.2807 | 5.8 | .0379 | .9705 |
| 2.0 | .0724 | 1.3067 | 6.0 | .0388 | .9782 |
| 2.2 | −.0245 | 1.3115 | 6.2 | .0373 | .9858 |
| 2.4 | −.1008 | 1.2990 | 6.4 | .0338 | .9929 |
| 2.6 | −.1562 | 1.2733 | 6.6 | .0292 | .9992 |
| 2.8 | −.1919 | 1.2385 | 6.8 | .0237 | 1.0045 |
| 3.0 | −.2098 | 1.1983 | 7.0 | .0180 | 1.0087 |
| 3.2 | −.2126 | 1.1561 | 7.2 | .0124 | 1.0117 |
| 3.4 | −.2031 | 1.1145 | 7.4 | .0072 | 1.0137 |
| 3.6 | −.1843 | 1.0758 | 7.6 | .0026 | 1.0146 |
| 3.8 | −.1593 | 1.0414 | 7.8 | −.0012 | 1.0148 |

## REFERENCES


1. Strang, W. J.: Transient Lift of Three-Dimensional Purely Supersonic Wing. Proc. Roy. Soc., Series A, June 22, 1950, pp. 54-80.

2. Miles, John W.: Transient Loading of Wide Delta Airfoils at Supersonic Speeds. Navord Rep. 1235, 1950.

3. Miles, John W.: On Harmonic Motion of Wide Delta Airfoils at Supersonic Speeds. Navord Rep. 1234, 1950.

4. Lomax, Harvard, Heaslet, Max. A., and Fuller, Franklyn B.: Three-Dimensional, Unsteady Lift Problems in High-Speed Flight - Basic Concepts. NACA TN 2256, 1950.

5. Jones, Arthur L., and Alksne, Alberta: The Load Distribution Due to Sideslip on Triangular, Trapezoidal, and Related Plan Forms in Supersonic Flow. NACA TN 2007, 1950.

6. Heaslet, Max. A., and Lomax, Harvard: Two-Dimensional Unsteady Lift Problems in Supersonic Flight. NACA Rep. 945, 1949.

7. Heaslet, Max. A., Lomax, Harvard, and Spreiter, John R.: Linearized Compressible-Flow Theory for Sonic Flight Speeds. NACA Rep. 956, 1950. (Formerly TN 1824)

8. Lagerstrom, P. A., and Graham, Martha E.: Low Aspect Ratio Rectangular Wings in Supersonic Flow. Douglas Aircraft Company, Inc. Rep. No. SM 13110, Dec. 1947.

9. Lomax, Harvard, Heaslet, Max. A., and Fuller, Franklyn B.: Formulas for Source, Doublet, and Vortex Distributions in Supersonic Wing Theory. NACA TN 2252, 1950.

10. Lomax, Harvard, and Sluder, Loma: Chordwise and Compressibility Corrections to Slender-Wing Theory. NACA TN 2295, 1951.

11. Stewartson, K.: Supersonic Flow Over an Inclined Wing of Zero Aspect Ratio. Proc. Cambridge Phil. Soc., vol. 46, pt. 2, April 1950, pp. 307-315.

12. Ribner, Herbert S.: The Stability Derivatives of Low-Aspect-Ratio Triangular Wings at Subsonic and Supersonic Speeds. NACA TN 1423, 1947.

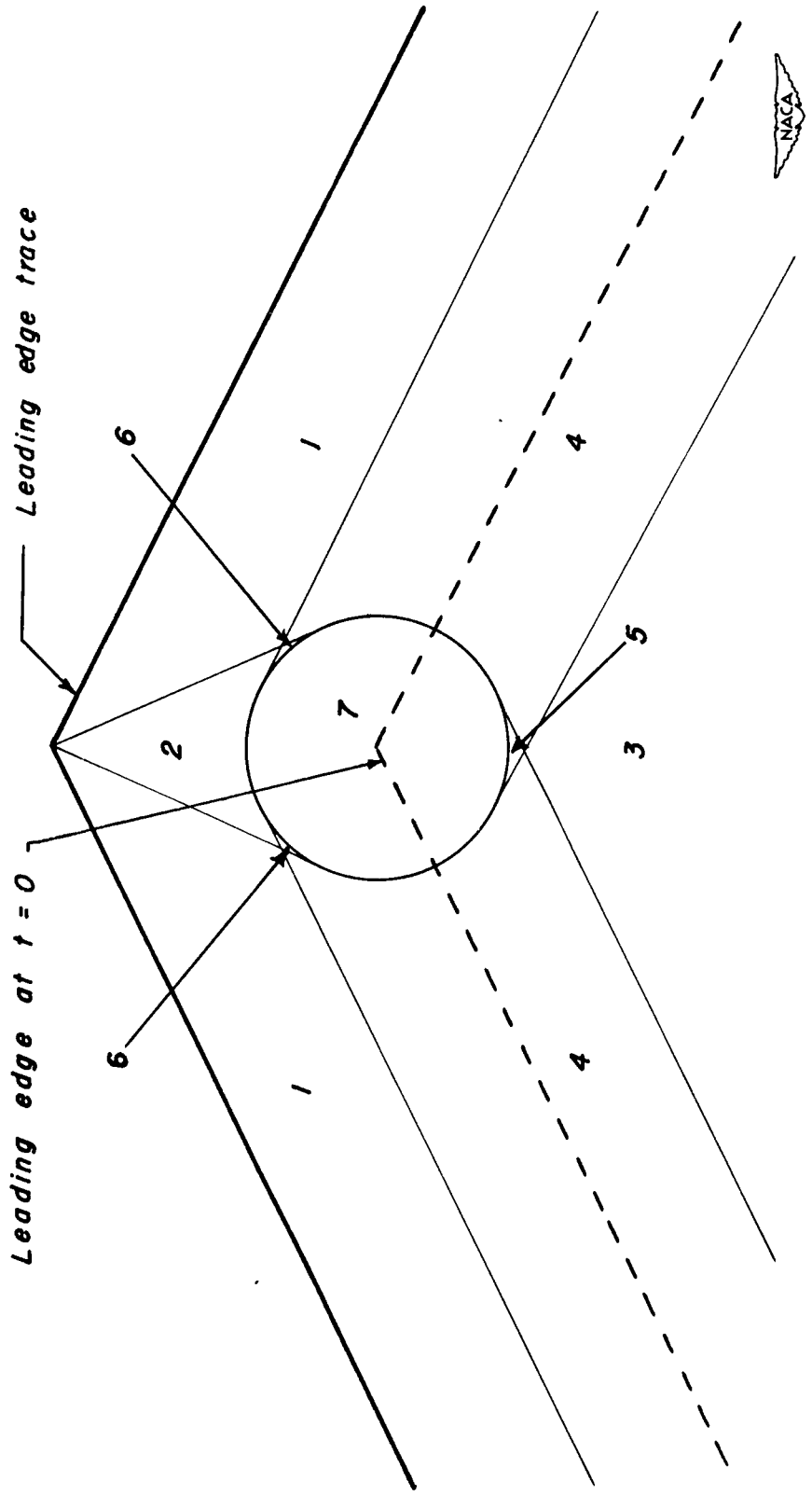


Figure 1.- The seven regions used in the analysis of the triangular wing with supersonic leading edges.

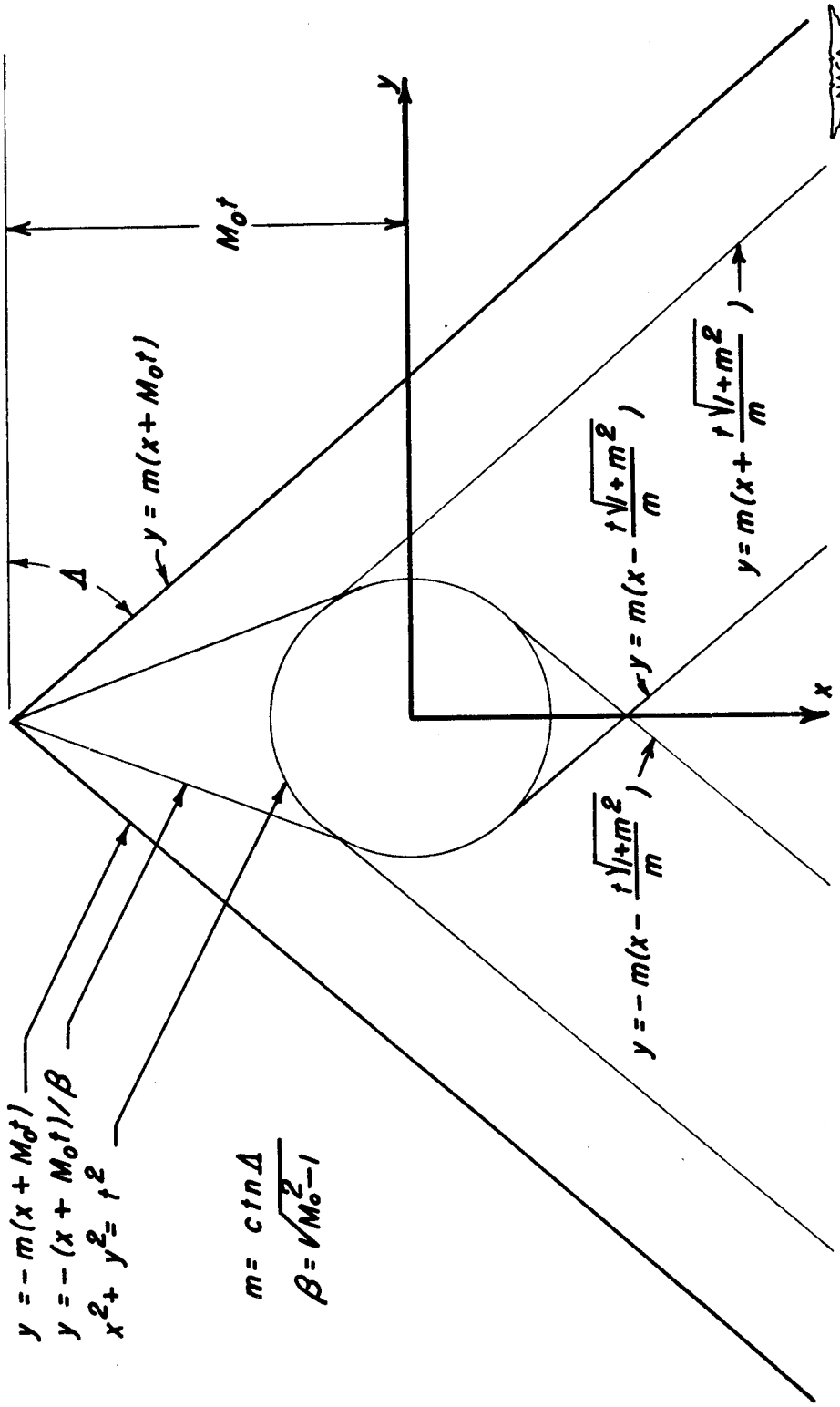


Figure 2.— Equations of lines pertinent to the analysis of the triangular wing with supersonic leading edges.

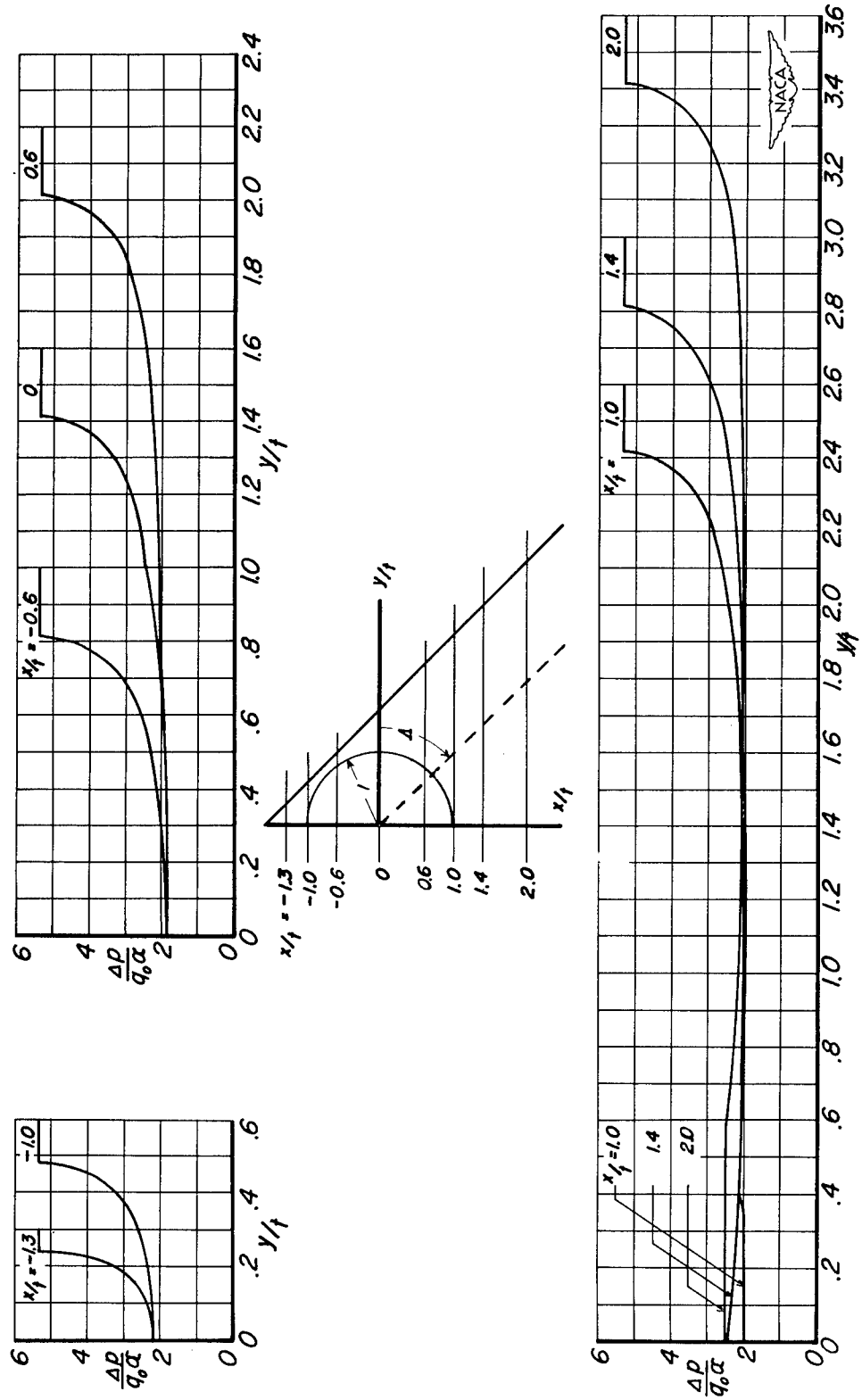


Figure 3.- Spanwise loading on sinking triangular wing with supersonic edges, $\Lambda = 45°$, $M_0 = 1.6$.

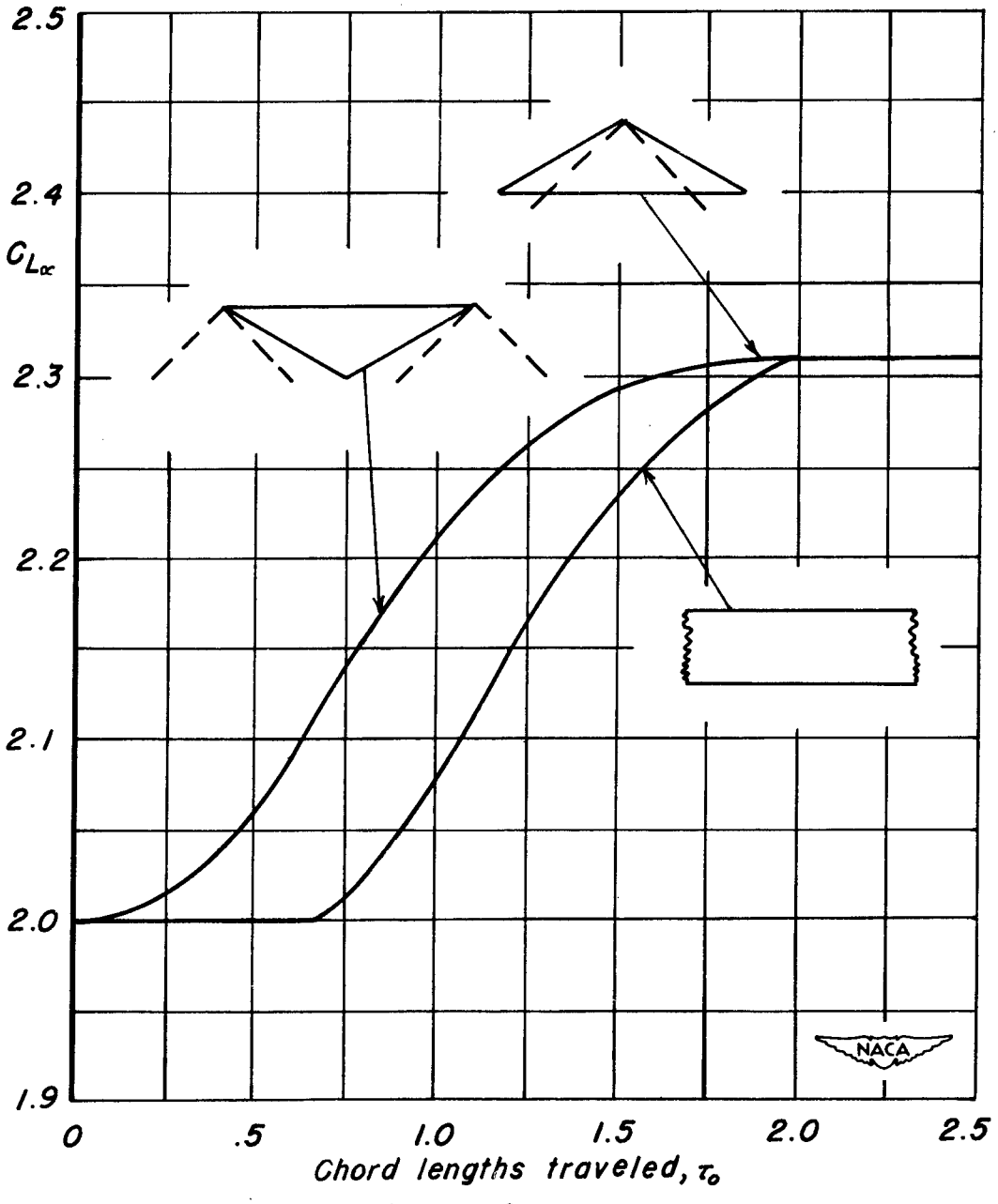


(a) Lift.

*Figure 4.- Indicial aerodynamic characteristics of sinking wings with supersonic leading edges. $M_o = 2$.*

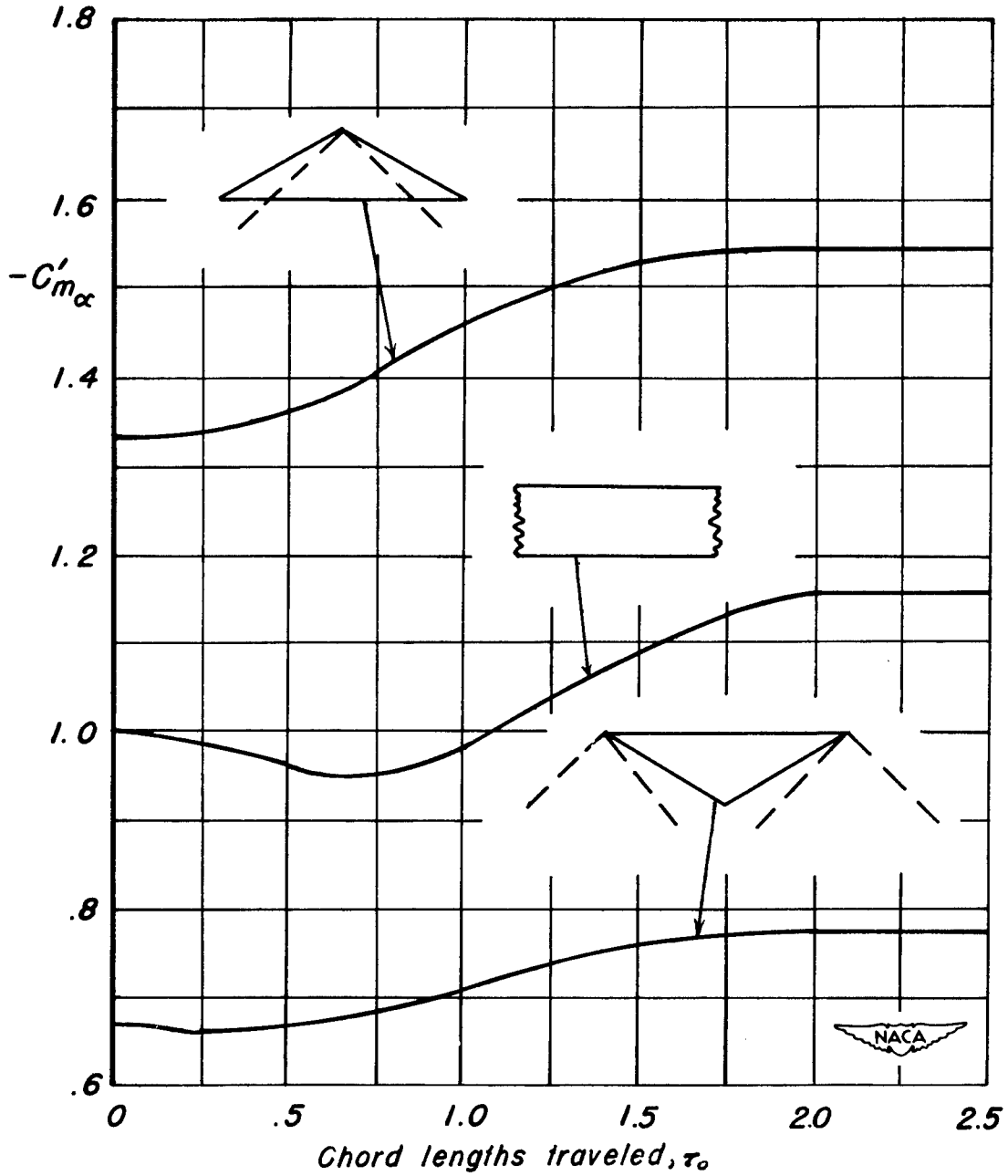


(b) Pitching moment about leading edge or apex.

Figure 4. – Continued.

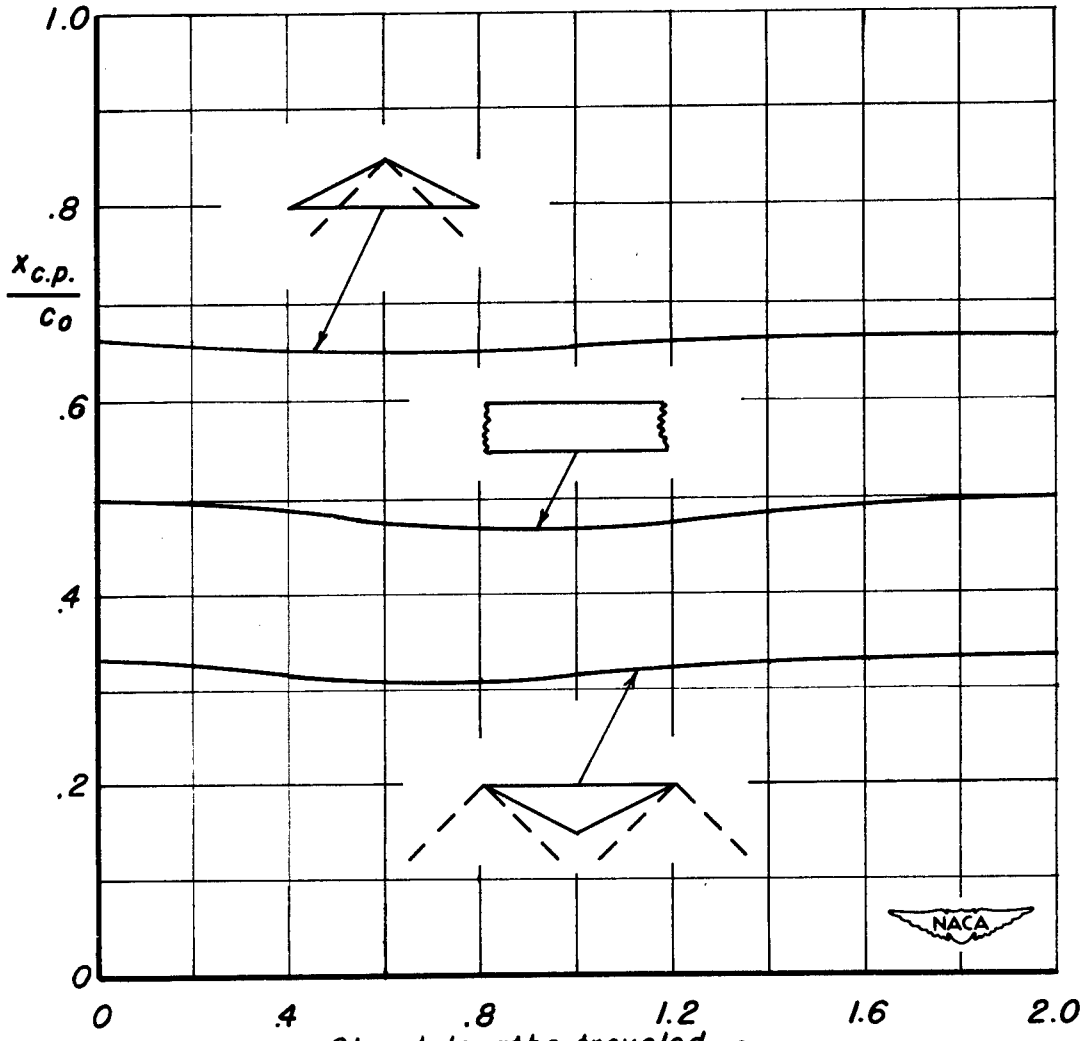


(c) Location of center of pressure with reference to the leading edge or apex.

Figure 4.– Concluded.

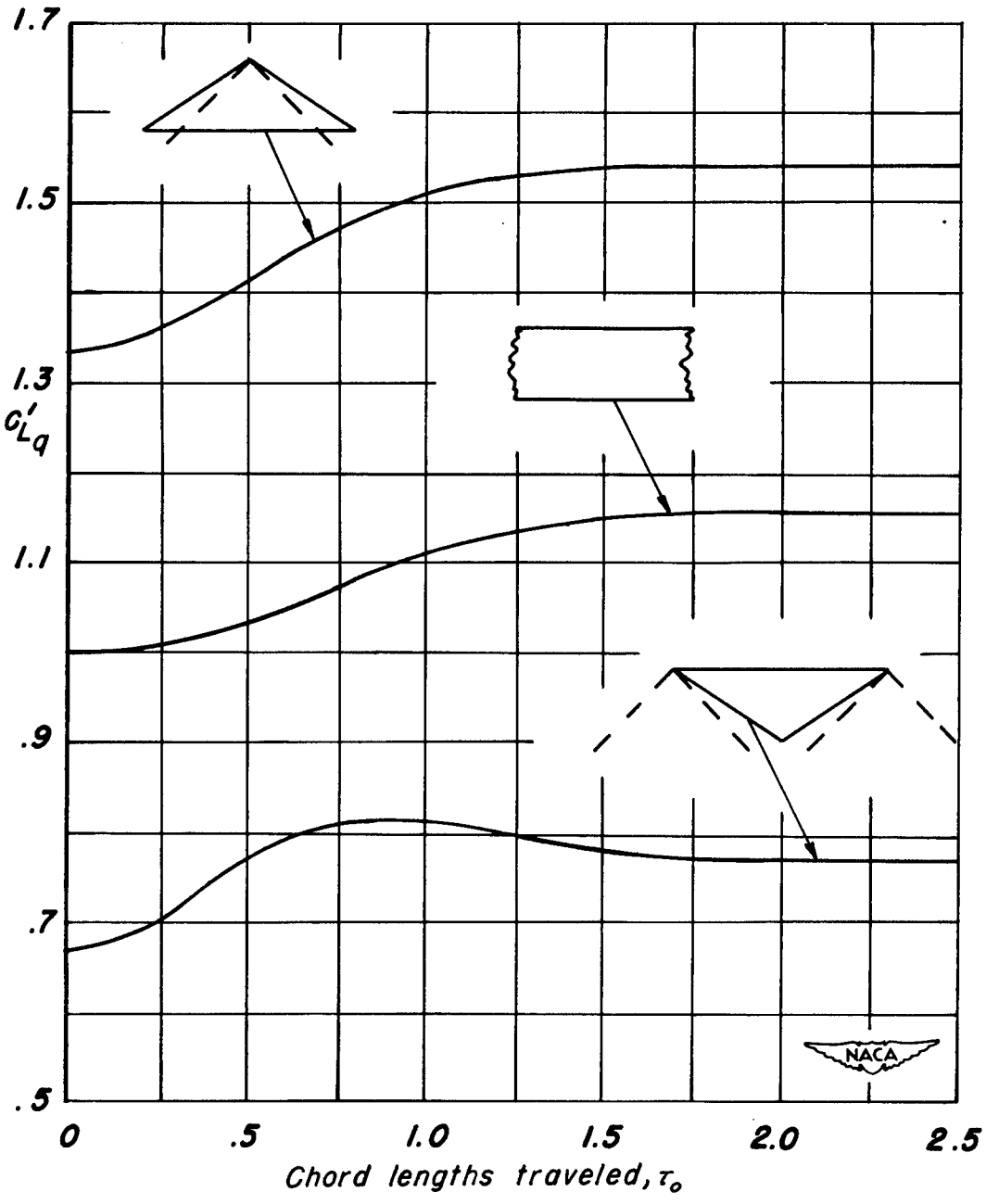


(a) Lift.

**Figure 5.– Indicial aerodynamic characteristics of wings with supersonic edges pitching about leading edge or apex. $M_o = 2$.**

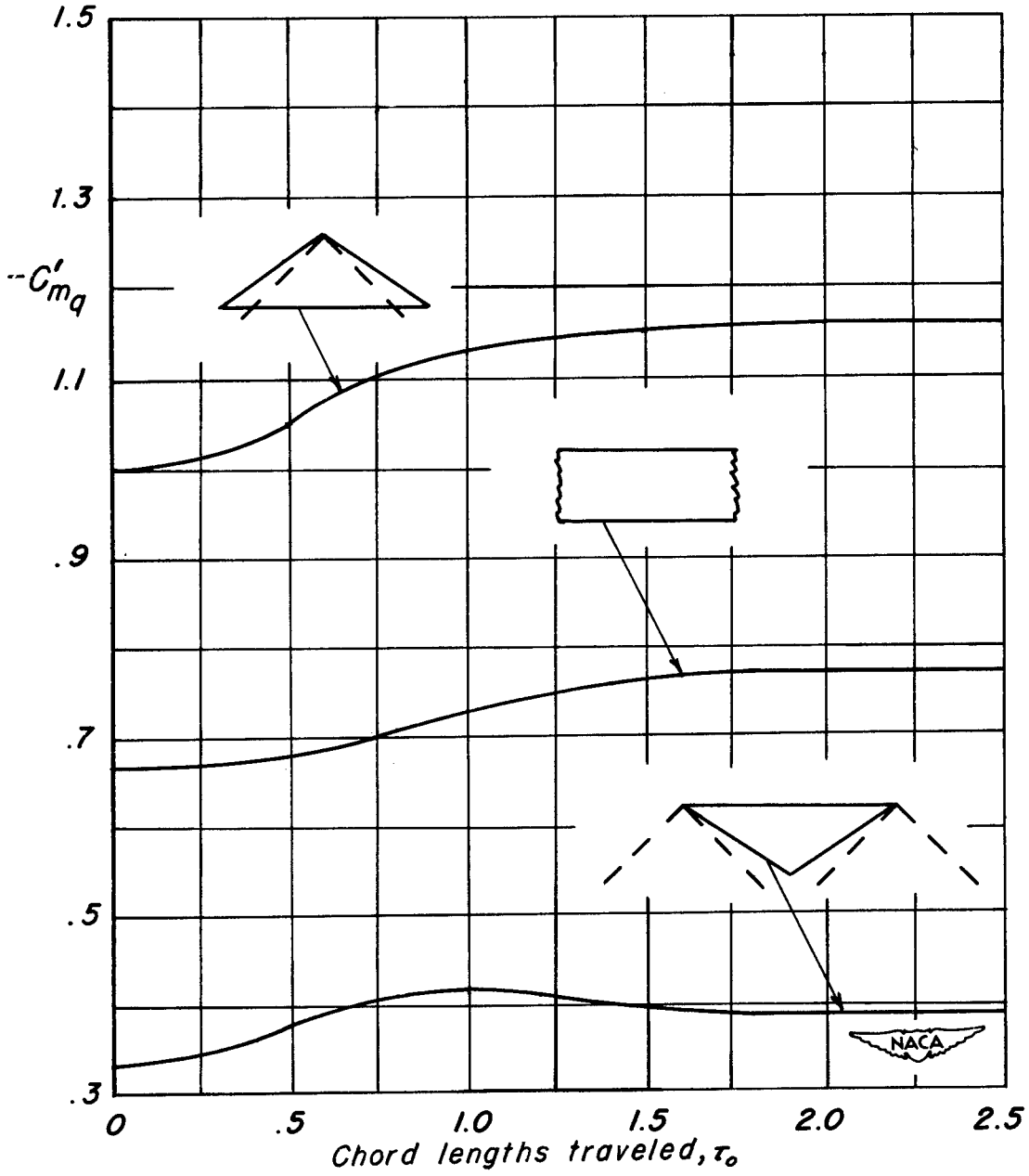


(b) Pitching moment about leading edge or apex.

Figure 5.- Continued.

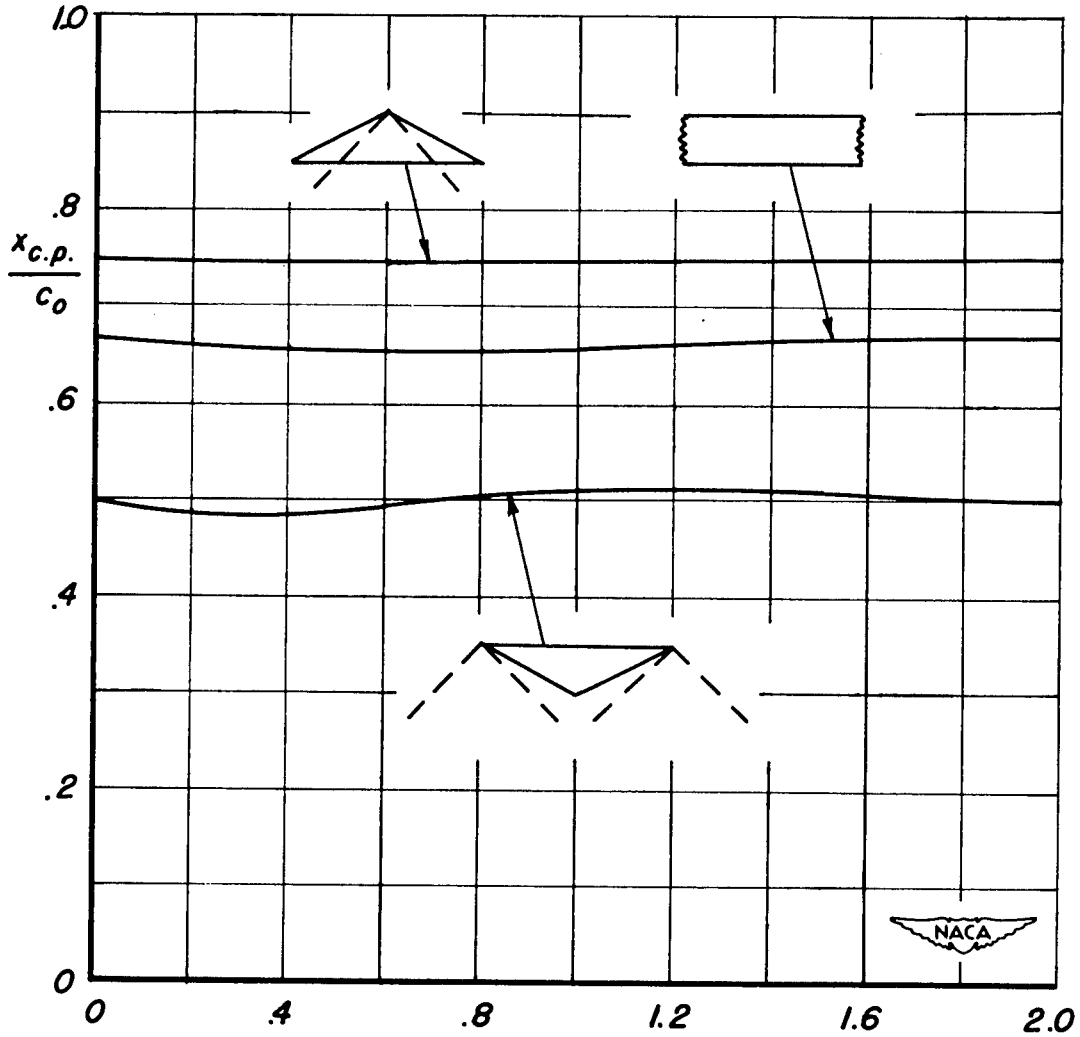


(c) Location of center of pressure with reference to the leading edge or apex.

Figure 5.- Concluded.

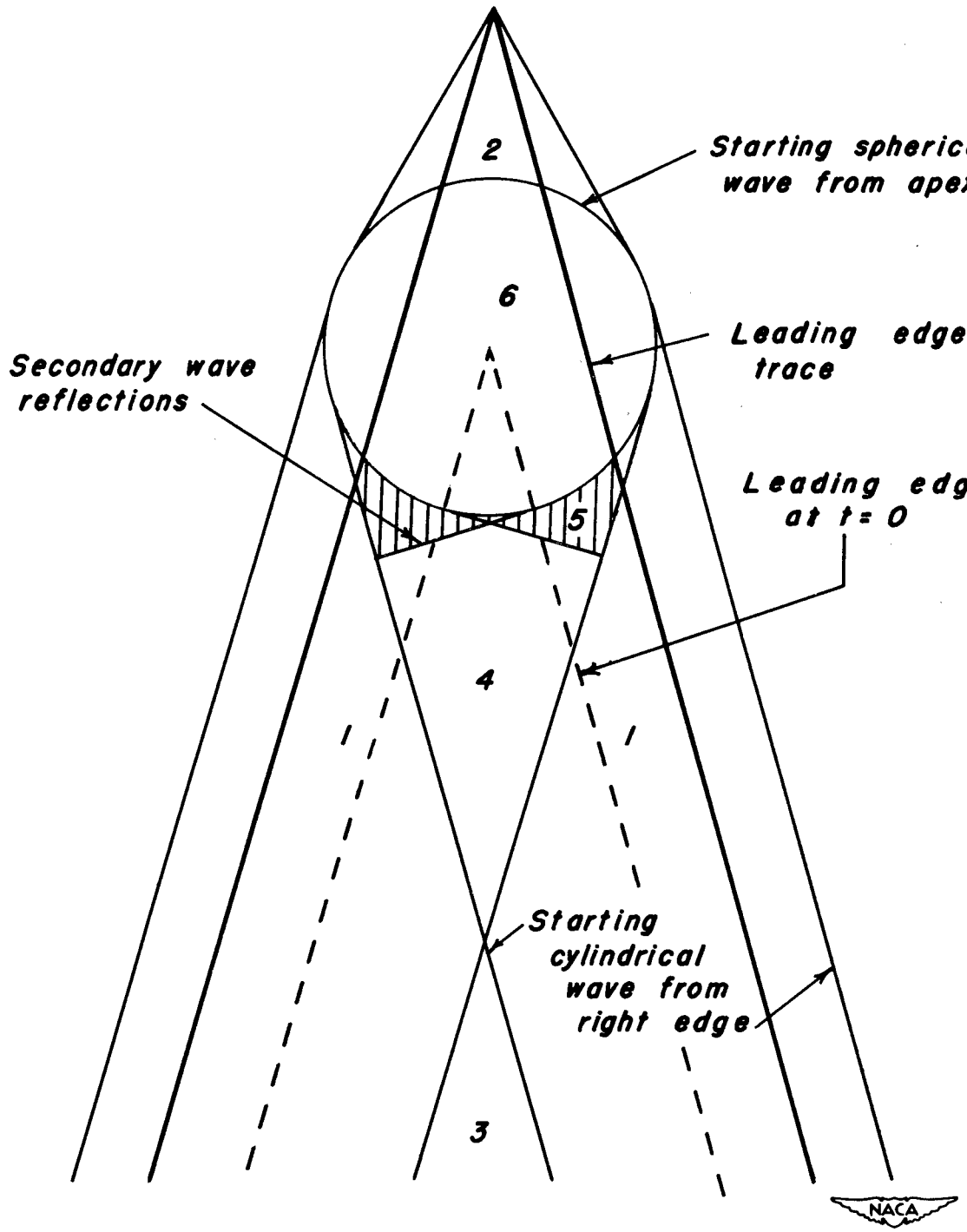


*Figure 6.– The six regions used in the analysis of the triangular wing with subsonic leading edges.*

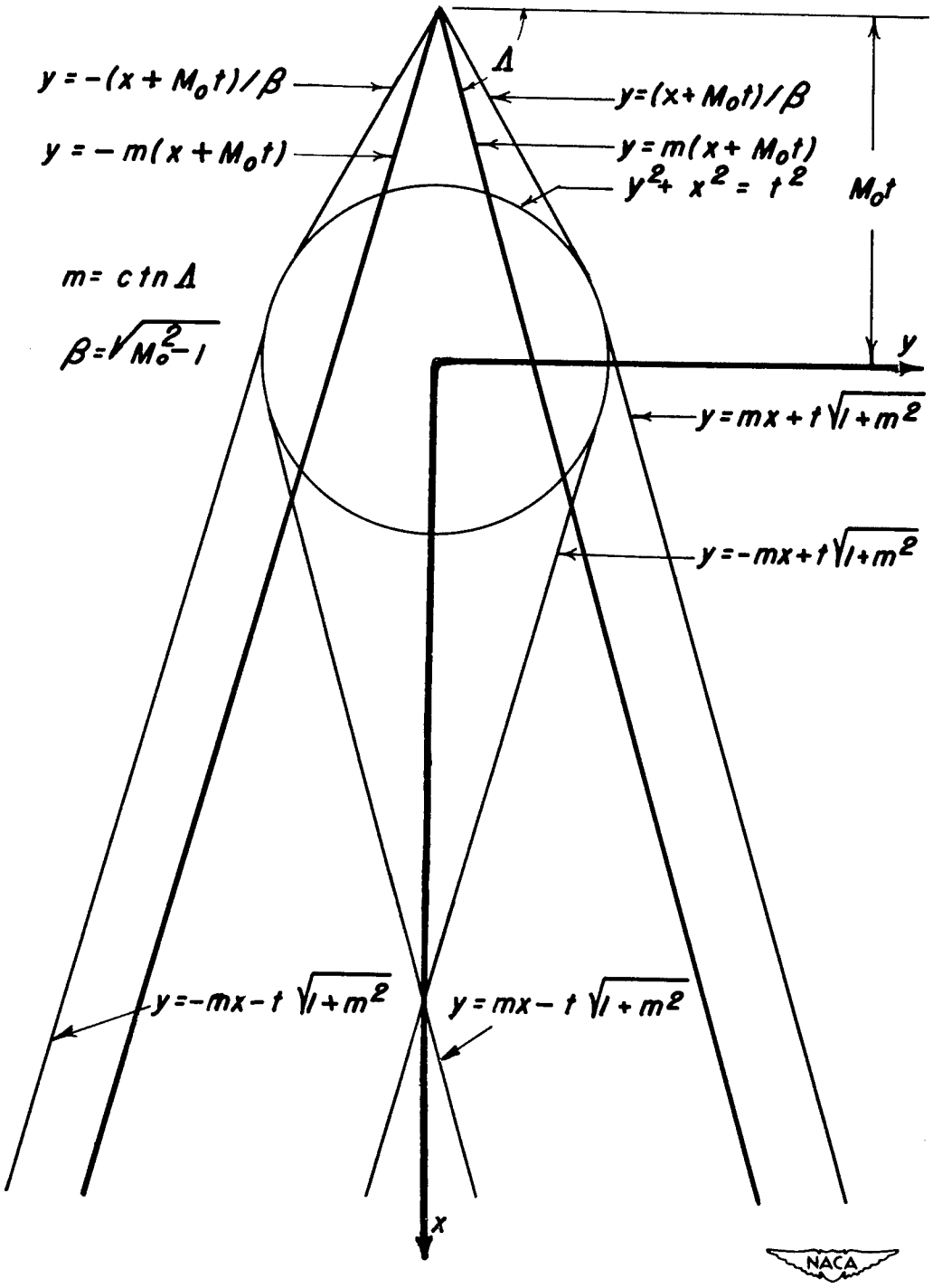


*Figure 7.– Equations of lines pertinent to the analysis of the triangular wing with subsonic leading edges.*

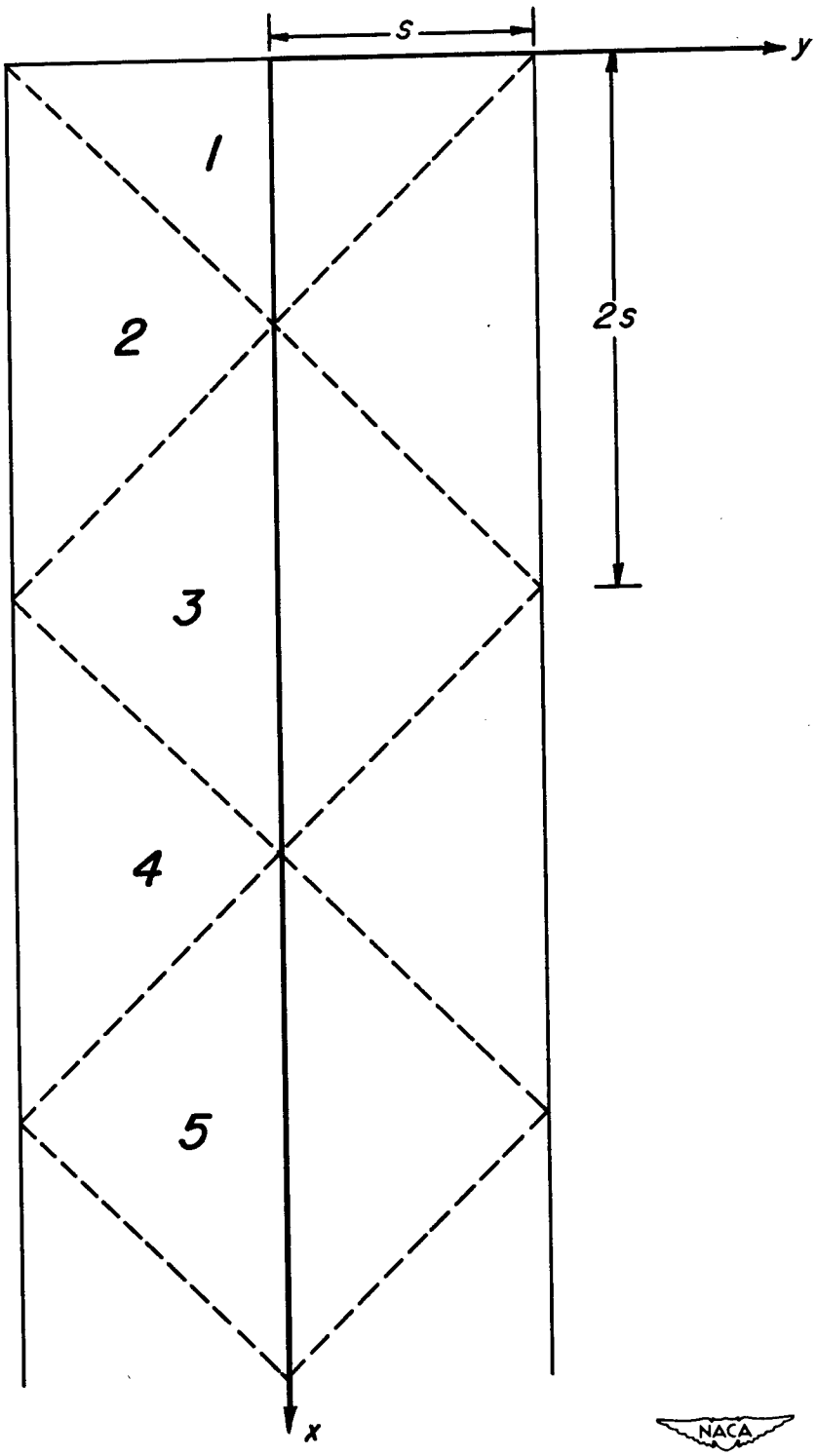


*Figure 8.– Regions used in the discussion of the low-aspect-ratio rectangular wing.*

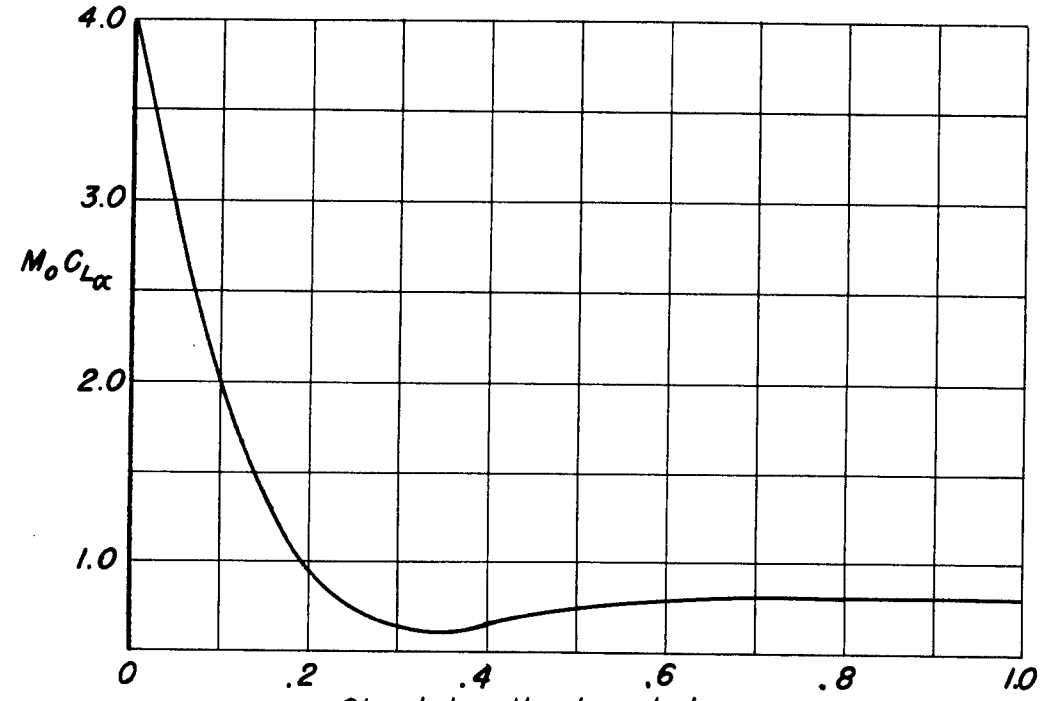


(a) Lift.

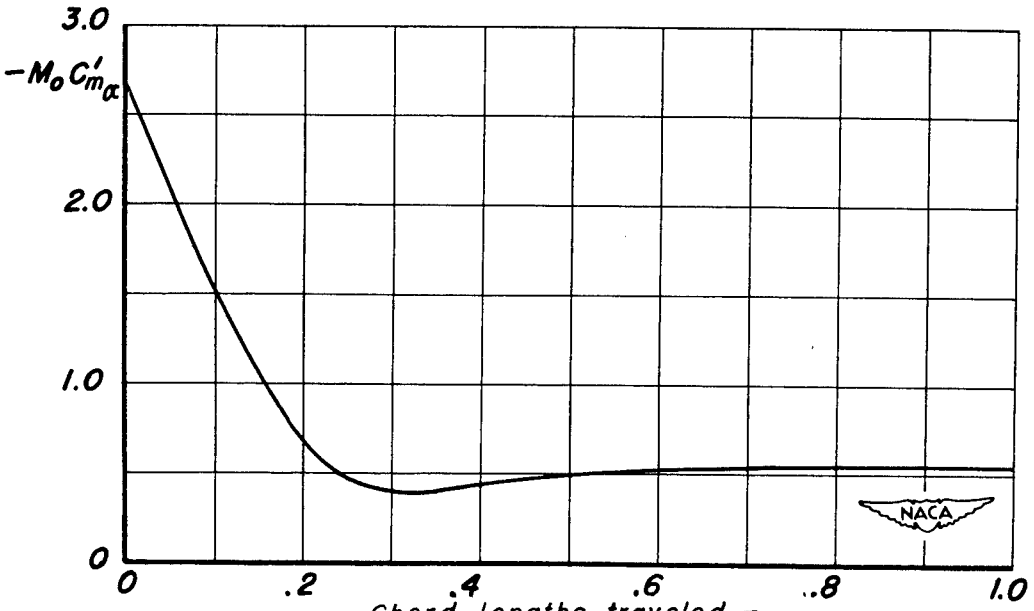


(b) Pitching moment about apex.

Figure 9.— Indicial aerodynamic characteristics of sinking triangular wings with slender plan forms. $mM_o = 1/8$.

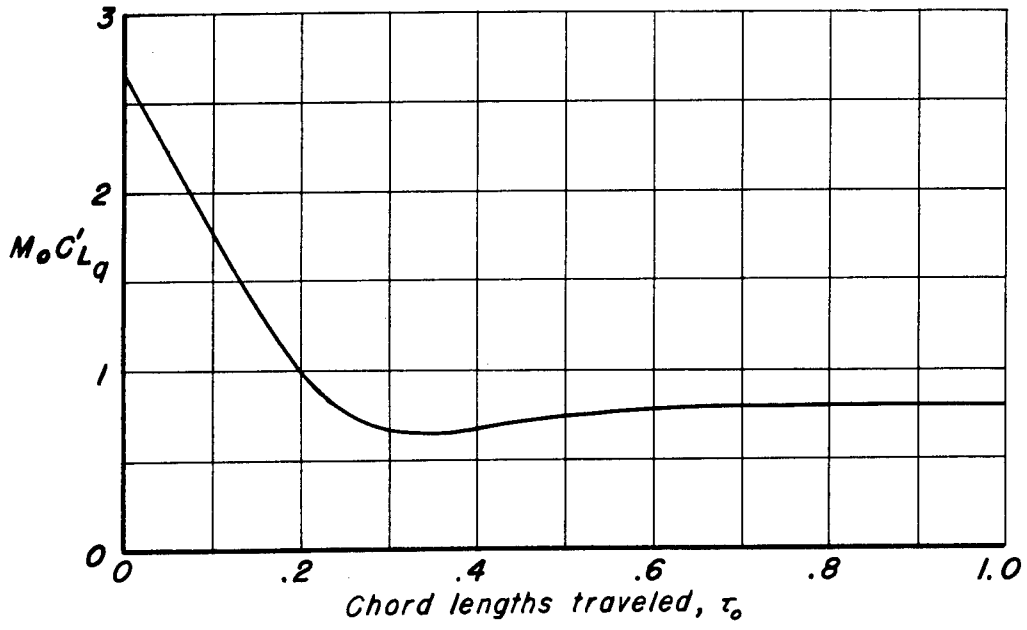


(a) Lift.

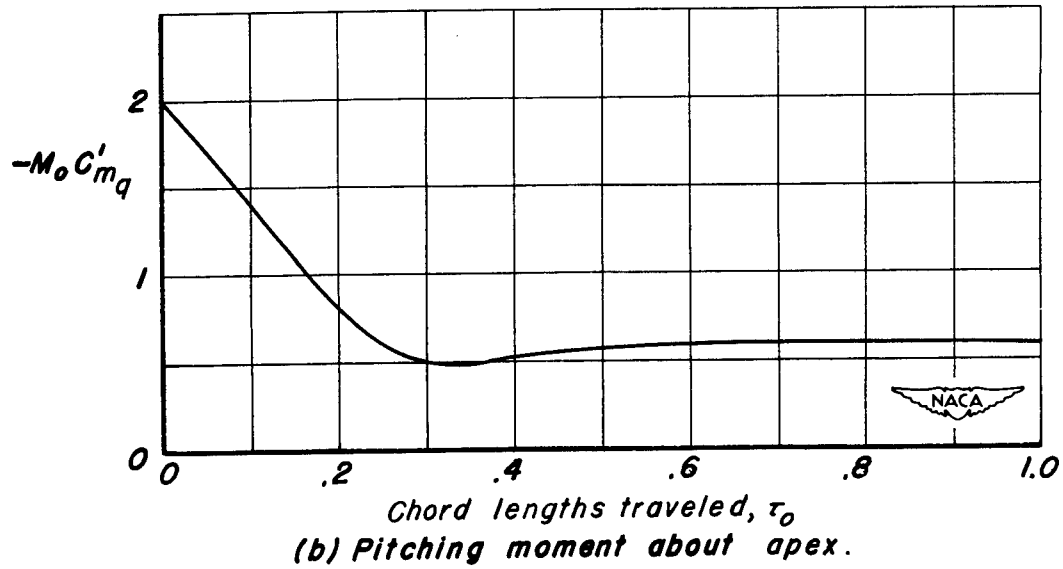


(b) Pitching moment about apex.

Figure 10.- Indicial aerodynamic characteristics of triangular wings with slender plan forms pitching about apex. $mM_o = 1/8$.

NACA TN 2387

National Advisory Committee for Aeronautics. THREE-DIMENSIONAL UNSTEADY LIFT PROBLEMS IN HIGH-SPEED FLIGHT - THE TRIANGULAR WING. Harvard Lomax, Max A. Heaslet and Franklyn B. Fuller. June 1951. 62p. diagrs. (NACA TN 2387)

The indicial lift and pitching-moment coefficients are derived for flat-plate triangular wings at supersonic speeds. Coefficients are determined for angle-of-attack distributions corresponding to sinking and pitching wings. The wing with supersonic edges is completely analyzed, the wing with subsonic edges is partially analyzed; the solution in this case being completed for very narrow wings by an application of slender wing theory. In case of the supersonic edges, a comparison is made with known two-dimensional results and also with results for the same triangular wing in reversed flow.

Copies obtainable from NACA, Washington

1. Wings, Complete - Theory (1.2.2.1)
2. Wings, Complete - Sweep (1.2.2.2.3)
3. Mach Number Effects - Complete Wings (1.2.2.6)
4. Stability, Longitudinal - Dynamic (1.8.1.2.1)
5. Damping Derivatives - Stability (1.8.1.2.3)
6. Loads, Maneuvering - Wings (4.1.1.1.2)

I. Lomax, Harvard
II. Heaslet, Maxwell Alfred
III. Fuller, Franklyn B.
IV. NACA TN 2387

NACA TN 2387

National Advisory Committee for Aeronautics. THREE-DIMENSIONAL UNSTEADY LIFT PROBLEMS IN HIGH-SPEED FLIGHT - THE TRIANGULAR WING. Harvard Lomax, Max A. Heaslet and Franklyn B. Fuller. June 1951. 62p. diagrs. (NACA TN 2387)

The indicial lift and pitching-moment coefficients are derived for flat-plate triangular wings at supersonic speeds. Coefficients are determined for angle-of-attack distributions corresponding to sinking and pitching wings. The wing with supersonic edges is completely analyzed, the wing with subsonic edges is partially analyzed; the solution in this case being completed for very narrow wings by an application of slender wing theory. In case of the supersonic edges, a comparison is made with known two-dimensional results and also with results for the same triangular wing in reversed flow.

Copies obtainable from NACA, Washington

1. Wings, Complete - Theory (1.2.2.1)
2. Wings, Complete - Sweep (1.2.2.2.3)
3. Mach Number Effects - Complete Wings (1.2.2.6)
4. Stability, Longitudinal - Dynamic (1.8.1.2.1)
5. Damping Derivatives - Stability (1.8.1.2.3)
6. Loads, Maneuvering - Wings (4.1.1.1.2)

I. Lomax, Harvard
II. Heaslet, Maxwell Alfred
III. Fuller, Franklyn B.
IV. NACA TN 2387